REVIEW

Check for updates

Photon upconversion sensitized by earth-abundant transition metal complexes

Pengyue Jin [ID] and Cui Wang [ID] *†

Sensitized triplet–triplet annihilation upconversion (sTTA-UC) converts two lower-energy absorbed photons into one emitting photon of higher-energy, and has become a popular approach for a wide range of applications. Current photosensitizers rely mostly on transition metal complexes made of expensive platinum group elements, such as palladium, platinum, and osmium, due to their strong absorption in the visible range, unity intersystem crossing, and long-lived triplet excited lifetimes. In recent years, fundamental breakthroughs have been made with photoactive complexes based on earth-abundant 3d metals including chromium, manganese, iron, cobalt, copper, and zinc, and 4d elements like zirconium and molybdenum. These novel complexes offer advantages, such as cost-effectiveness, sustainability, low toxicity, scalability for industrial use, and potential for innovative research in areas including catalysis and energy conversion, making them promising alternatives to noble metal-based photosensitizers in sTTA-UC and other fields. In this review, we delineate the recent advancements in sTTA-UC utilizing photoactive earth-abundant transition metal complexes. We explore their energy transfer mechanisms, evaluate their upconversion performance, discuss their applications, and outline the challenges and perspectives, aiming to offer insights for the development of novel photosensitizers based on earth-abundant metals for future research and applications.

Introduction

Sensitized triplet–triplet annihilation upconversion (sTTA-UC) converts two low-energy absorbed photons into one higher-energy photon under non-coherent light excitation.[1–4] This biphotonic process has attracted significant interest in many fields, including biosensing/imaging,[5–12] photovoltaics,[13–17] organic light-emitting diodes (OLEDs),[18–20] photocatalysis,[15,21–36]

Department of Biology and Chemistry, Osnabrück University, Barbarastraße 7, Osnabrück 49076, Germany. E-mail: cui.wang@uni-konstanz.de

† Current address: Department of Chemistry, University of Konstanz, Universitätsstraße 10, Konstanz 78464, Germany.

Pengyue Jin received his BEng in Environmental Science from Shanxi University in 2020. Then he continued his Master's degree at Sichuan University and conducted his Master's thesis under the supervision of Prof. Dr Cheng Yang. He joined Cui Wang's group as a PhD student at Osnabrück University March 2024, and moved with Cui to the University of Konstanz April 2025.

Pengyue Jin
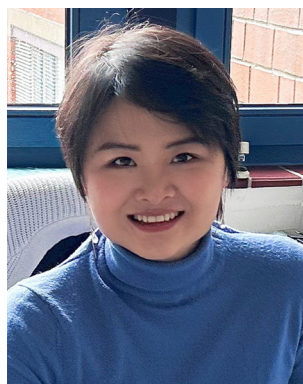
Cui Wang received her MSc in Chemistry from the Free University of Berlin in 2017 and obtained her Dr. rer. nat. degree in 2021 in Berlin under the supervision of Ute Resch-Genger at the Federal Institut of Materials Research and Testing (BAM). After the postdoctoral research with Oliver S. Wenger at the University of Basel, in 2023 she started an independent research group at Osnabrück University as an assistant professor (W1). Since 2025 she has been a tenure-track professor in inorganic chemistry at the University of Konstanz.

Cui Wang

This journal is © the Owner Societies 2025

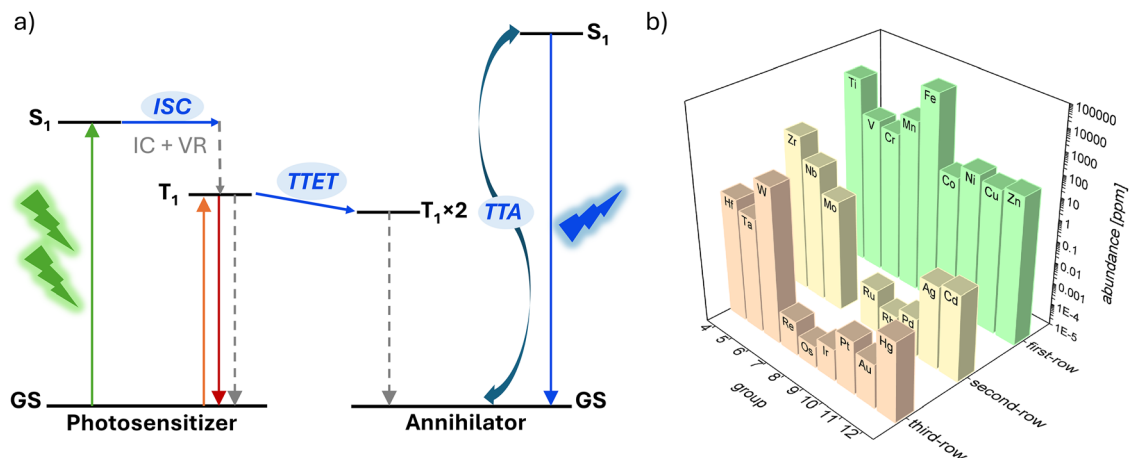*Phys. Chem. Chem. Phys.*, 2025, **27**, 13793–13811 | 13793

Fig. 1 (a) Energy level diagram illustrating sTTA-UC sensitized by a triplet photosensitizer. The green and orange arrows indicate the $S_0 \rightarrow S_1$ and $S_0 \rightarrow T_1$ absorption, respectively. ISC: intersystem crossing, IC: internal conversion, VR: vibrational relaxation, TTET: triplet–triplet energy transfer, TTA: triplet–triplet annihilation. (b) Logarithmic plot of the abundance of transition metals in the Earth's crust.

among others.[37] Molecular sTTA-UC relies on the bimolecular interplay between a photosensitizer and an annihilator.[10,16,22,38] As shown in Fig. 1a, triplet photosensitizers are often used for triplet–triplet energy transfer (TTET) to the energetically lowest triplet state (T_1) of an annihilator, from which triplet–triplet annihilation (TTA) subsequently occurs. This leads to one annihilator released to the ground state and another one populated in the singlet state (S_1), from which a photon of higher energy than the absorbed ones is emitted with a delayed nature of μs-scaled lifetimes.[2–4,21,39] Key performance parameters for sTTA-UC include the pseudo anti-Stokes shift ΔE, the upconversion quantum yield Φ_{UC}, and the excitation power density threshold I_{th}. The ΔE refers to the energy gap between the wavelengths of the excitation and the upconversion luminescence maximum (eqn (1)).

$$\Delta E \text{ (eV)} = E_{UC} - E_{exc} \qquad (1)$$

To maximize the ΔE, the energy lost caused by the $S_1 \rightarrow T_1$ transition can be suppressed by employing photosensitizers with small S_1–T_1 energy gaps, such as the thermally activated delayed fluorescence (TADF) fluorophores.[40–46] Recent achievements show that this energy loss can be circumvented by using photosensitizers featuring direct $S_0 \rightarrow T_1$ absorption allowed by the strong spin–orbit coupling (Fig. 1a, orange arrow), as typically seen with osmium(II) complexes.[47–52]

The upconversion quantum yield (Φ_{UC}) describes the overall efficiency of converting the input photons absorbed by the photosensitizer to the upconverted emission photons from the annihilator. Φ_{UC} depends on the quantum efficiencies of the involved processes, i.e. intersystem crossing (ISC) of the photosensitizer, TTET, TTA, and the fluorescence (Φ_{FL}) of the annihilator, as expressed by eqn (2).[53,54]

$$\Phi_{UC} = \frac{1}{2}f \cdot \Phi_{ISC} \cdot \Phi_{TTET} \cdot \Phi_{TTA} \cdot \Phi_{FL} \qquad (2)$$

In this equation, the factor $\frac{1}{2}$ indicates the theoretical maximum of 50% for biphotonic sTTA-UC.[54] f is the spin-statistical factor for generating one singlet spin-state via TTA. Annihilation

of two triplet excited chromophores yields nine spin states, including one singlet, three triplet, and five quintet states.[53] This leads to a maximum spin-statistical factor f_{max} of 1/9 (11.1%) for forming the singlet state that gives the upconversion luminescence and therefore a maximal Φ_{UC} of 5.5%. Recent studies found that the f factor depends on the energy levels of the T_1, T_2, and S_1 states for the annihilator, and $f_{max} \sim$ 40% ($\Phi_{UC,max} \sim 20\%$) becomes achievable when both the singlet and triplet channels are open.[46,53,55,56]

Another essential performance parameter for sTTA-UC is the excitation power density threshold (I_{th}), which indicates the transition of the quadratic dependence of the upconversion luminescence on the excitation power density to a linear regime.[4,57,58] I_{th} marks the point when TTA becomes the dominant reaction pathway for the triplet excited state of the annihilator.[57,59] I_{th} is affected by the inherent triplet excited state decay (k_T) of the annihilator, the TTA rate constant (k_{TTA}), the absorption cross-section (α) at the excitation wavelength as well the concentration [PS] of the photosensitizer, and the TTET efficiency (Φ_{TTET}), as shown in eqn (3).[46] Common strategies for lowering the I_{th} value include extension of the triplet excited state lifetime of the photosensitizer for efficient TTET[28] and enhancement of the photosensitizer absorbance at the excitation wavelength.[35,57]

$$I_{th} = \frac{k_T^2}{2k_{TTA} \cdot \alpha \cdot [PS] \cdot \Phi_{TTET}} \qquad (3)$$

In comparison with the well-known lanthanide-based upconversion (UC) systems, molecular sTTA-UC is often beneficial due to the relatively lower excitation power densities,[15,60] the substantially larger absorption coefficients of the photosensitizers than lanthanide absorbers like Yb(III) or Nd(III),[61,62] the relatively high achievable Φ_{UC}, and the tunable wavelengths of the excitation source and the delayed fluorescence by the choice of photosensitizer/annihilator combinations.[4,21,63] Oxygen quenching of the involved triplet states in sTTA-UC dramatically abates the Φ_{UC}, but this issue can now be addressed by

13794 | Phys. Chem. Chem. Phys., 2025, 27, 13793–13811

This journal is © the Owner Societies 2025

encapsulating the chromophores into nanoconfinements[64,65] or employing deoxygenating solvents.[35,36,66]

To date, triplet photosensitizers featuring excited state properties favorable for efficient sTTA-UC are mostly based on precious platinum metal complexes (Fig. 1b), such as Pd(II), Pt(II),[66–74] Ru(II),[35,75–78] Ir(III),[28,79,80] and Os(II).[22,47,48,81–83] However, the use of expensive heavy metals makes these photosensitizers less attractive, due to the high cost, scarcity, environmental damage, toxicity, and over-reliance risks. This leads to the desire for more sustainable and cost-effective alternatives. There has recently been enormous interest in the development of organic triplet photosensitizers for sTTA-UC, such as doublet organic radicals,[84–86] TADF fluorophores with small S_1–T_1 energy gaps,[40–45] and organic triplet photosensitizers based on the spin–orbit charge transfer intersystem crossing,[87–89] as summarized in recent reviews.[38,90] Photosensitizers based on earth-abundant transition metals are furthermore seen as attractive alternatives for sTTA-UC (Fig. 1b).

In recent years, remarkable achievements have been made with photoactive coordination compounds based on earth-abundant transition metals,[91–99] including vanadium,[100–104] chromium,[29,105–114] manganese,[115–119] iron,[117,120–130] cobalt,[131–134] nickel,[135–140] copper,[141–151] zinc,[152–154] zirconium,[155,156] and molybdenum.[157–162] These fundamentally new metal complexes are considered as more sustainable substitutes for the well-known photosensitizers made of precious metals mentioned above.[163–165] Using photoactive earth-abundant metal complexes for sTTA-UC is raising increasing interest, although in many cases their performance in upconversion is inferior to precious metal-based photosensitizers. This is mainly attributed to the fundamental challenges associated with the intrinsic

photophysical properties of these complexes and the underexplored energy transfer mechanisms.

This review summarizes the sTTA-UC systems sensitized by earth-abundant metal complexes with focus on their unusual energy transfer mechanisms, the upconversion performance, and the applications based on these sTTA-UC systems. Our objective is to provide a comprehensive analysis that not only underscores the potential of using photoactive earth-abundant metal complexes for the sTTA-UC field, but also underlines the underexplored energy transfer mechanisms that are fundamentally important for photochemistry.

Photon upconversion sensitized by earth-abundant metal complexes and its applications

Herein, we provide an overview of the recent developments of using earth-abundant transition metal complexes as photosensitizers for sTTA-UC, including several photoactive first-row transition metal complexes based on $3d^3$ Cr(III),[112,166] $3d^5$ Fe(III),[31,36,130] $3d^6$ Cr(0)[27,167] and Mn(I),[116] $3d^{10}$ Cu(I)[141,144] and Zn(II),[152,168–174] and two second-row $4d^0$ Zr(IV)[175] and $4d^6$ Mo(0)[157,158] metal complexes. The key relevant photophysical parameters of these photosensitizers are summarized in Table 1, and their performance parameters for sTTA-UC are given in Table 2. Additionally, further applications based on these sTTA-UC, such as photocatalysis, are discussed.

$3d^3$ Cr(III) complexes

Important processes have recently been made with mononuclear luminescent $3d^3$ Cr(III) complexes with tridentate polypyridyl

Table 1 Key photophysical parameters of the photosensitizers based on earth-abundant metal complexes used for sTTA-UC

Photosensitizer	$\lambda_{abs}{}^a$ [nm]	$\lambda_{em}{}^a$ [nm]	$E_{D/T}{}^b$ [eV]	$\Phi_{PL}{}^c$ [%]	$\tau_{PL}{}^d$ [ns]	$\tau_{T,dark}{}^e$ [μs]	Literature
[Cr(bpmp)$_2$](PF$_6$)$_3$	465	709	1.75	—	890 000	—	166
[Cr$_2$(dNinp)$_2$(μ-OH)$_2$(μ-O$_2$CMe)](OTf)$_3$	500	728	1.70	0.01	450	—	112
[Fe(ImPP)$_2$](PF$_6$)	635	725	1.71	0.07	0.267	—	31
[Fe(CNAnt$_2$)$_2$](Br)	635	725	1.82	0.08	98	—	130
[Fe(phtmeimb)$_2$](PF$_6$)	502	670	2.13	1.82	1.60	—	36
[Cr(CN^{t}BuAr$_3$NC)$_3$]	500	630	2.05	0.001	2.2	—	167
[Cr(L^{pyr})$_3$]	550	740	1.67	0.66	24	—	27
[Mn(L^{tri})$_2$](PF$_6$)	400	525	2.3	0.03	1.73	—	116
[Cu(dsbtmp)$_2$](PF$_6$)	∼450	630	1.97	—	2800	—	141
[Cu(dsbp)$_2$](PF$_6$)	∼460	690	1.80	—	400	—	141
ZnTPTBP	655	729	—	0.2	1.4	155.7	170
ZnTPPOH	421	660	—	—	—	11 000	172
F$_{16}$ZnPc	—	—	1.40	—	—	—	173
ZnTPP	549	646	1.59	3.3	—	1900	23, 168 and 171
[Zn(m-L)$_2$]	419	504	—	50	25	38	152
ZnBDP-An	491	518	—	0.7	1.6	295	174
ZnBDP-Pyr	489	517	—	0.4	0.9	146	174
Zr(^{Mes}PDP^{Ph})$_2$	525	581	1.93	—	350 000	—	175
[Mo(L^{DMB})$_2$]	550	720	1.94	1.5	54	—	157
[Mo(CO)$_3$(tpe)]	473	715	1.72	0.66	355	—	158

^{a} λ_{abs} and λ_{em} are the wavelengths of the energetic lowest absorption band maximum and the luminescence peak, respectively. ^{b} $E_{D/T}$ stands for the doublet or triplet excited state energy level of the given photosensitizer for energy transfer to the annihilator. ^{c} Φ_{PL} is the photoluminescence quantum yield. ^{d} τ_{PL} is the photoluminescence lifetime. ^{e} $\tau_{T,dark}$ is the dark triplet state lifetime. The solvent used for determining the above photophysical parameters is consistent with the solvent used for photon upconversion studies.

This journal is © the Owner Societies 2025

Phys. Chem. Chem. Phys., 2025, **27**, 13793–13811 | **13795**

Table 2 Qualification parameters for sTTA-UC sensitized by earth-abundant metal-based complexes

Photosensitizer	Annihilator (mediator)	$\Phi_{\text{DTET/TTET}}$ [%]	Φ_{UC}^{a} [%]	I_{th} [W cm^{-2}]	$\lambda_{\text{exc}}/\lambda_{\text{UCL}}$ [nm]	ΔE [eV]	Ref.
[Cr(bpmp)$_2$](PF$_6$)$_3$	DPA	>90	12	1.56	532/432	0.54	166
[Cr$_2$(dNinp)$_2$(μ-OH)$_2$(μ-O$_2$CMe)](OTf)$_3$	AnTIPS	—	—	—	532/470	0.31	112
[Fe(ImPP)$_2$](PF$_6$)	BPEA	4	0.019	46	635/508	0.52	31
[Fe(CNAnt$_2$)$_2$](Br)	BPEA	94	1.30	1.4	635/508	0.52	130
[Fe(phtmeimb)$_2$](PF$_6$)	An	12.3	0.003	—	532/407	0.72	36
	PhAn	14.5	0.06	52.3	532/420	0.62	36
	PhAn(An)	—	0.04	—	532/420	0.62	36
	DPA	22.5(22.9)	0.03	—	532/435	0.52	36
	DPA(An)	—	0.19	—	532/435	0.52	36
	DPA(PhAn)	—	0.16	—	532/435	0.52	36
[Cr(CN^{t}BuAr$_3$NC)$_3$]	An	—	—	—	530/405	0.72	167
[Cr(L$^{\text{pyr}}$)$_3$]	AnTIPS	∼40	1.8	5.9	705/470	0.88	27
[Mn(L$^{\text{tri}}$)$_2$](PF$_6$)	An	12.1	—	—	420/∼410	∼0.07	116
[Cu(dsbtmp)$_2$](PF$_6$)	An	>90	0.46	—	488/384	0.69	141
	DMA	>90	4.6	—	488/410	0.48	141
	DPA	>90	8.9	—	488/414	0.45	141
	PAC	—	—	7.73	488/∼410	∼0.48	144
[Cu(dsbp)$_2$](PF$_6$)	An	>90	0.34	—	488/404	0.53	141
ZnTPTBP	Per-Bodipy	—	0.38	—	654/545	0.38	170
	Perylene	—	0.16	—	654/450	0.86	170
ZnTPPOH	TBPer	>90	12	0.359	532/∼470	0.31	172
F$_{16}$ZnPc	PDI-CH$_3$	—	—	—	700/—	—	173
ZnTPP	ZnTPP	—	—	—	532/∼430	0.55	23, 168 and 171
[Zn(m-L)$_2$]	Naph-Tips	—	0.73	—	430/∼370	0.47	152
ZnBDP-An	Perylene	—	3.05	—	510/∼450	0.33	174
ZnBDP-Pyr	Perylene	—	1.65	—	510/∼450	0.33	174
Zr($^{\text{Mes}}$PDP$^{\text{Ph}}$)$_2$	DPA	95	21.35	—	514.5/∼404	0.66	175
	CzPA	95	18.7	—	514.5/∼413	0.59	175
	F-CzPA	95	18.9	—	514.5/∼413	0.59	175
	CN-CzPA	95	15.85	—	514.5/∼426	0.50	175
[Mo(L$^{\text{DMB}}$)$_3$]	DPA	36	1.8	—	635/430	0.93	157
[Mo(CO)$_3$(tpe)]	DPA	85	12	0.09	514/435	0.44	158

^{a} Theoretical maximal Φ_{UC} is set to 50%.[54]

ligands, the so-called molecular rubies. Many of the spin–flip doublet excited states of these novel Cr(III) complexes show high luminescence quantum yields and extremely long lifetimes up to the ms-scale,[107–109,176,177] due to the large ligand field splitting with strongly σ-donating and π-accepting ligands and almost perfectly octahedral geometry,[105–109,176,178,179] and some of them exhibit high excited state redox potentials.[180–182] These photophysical and photochemical properties make the photoactive Cr(III) complexes attractive for applications relying on energy- and electron-transfer processes,[180–188] such as energy transfer or photoredox catalysis.

Among the highly luminescent molecular rubies, [Cr(bpmp)$_2$]$^{3+}$ (bpmp = 2,6-bis(2-pyridylmethyl)pyridine) exhibits at room temperature bright phosphorescence maximized at 709 nm with a near millisecond lifetime from the ^{2}E/^{2}T$_1$ spin–flip excited states (Table 1).[166] In the presence of 9,10-diphenylanthracene (DPA, Fig. 2a), it was found that an unusual doublet-triplet energy transfer (DTET) occurs from the ^{2}E/^{2}T$_1$ excited states of the Cr(III) complex to the T$_1$ state of DPA with similar energy levels (Fig. 2c). The small energy gap between these excited states makes the DTET thermodynamically feasible, but also reversible to some extent. Importantly, the DTET is a spin-allowed process according to the Wigner spin conservation rule,[189,190] because the total spin of the [Cr(bpmp)$_2$](PF$_6$)$_3$/DPA pair remains unchanged (Fig. 2b). The DTET process was experimentally evidenced with steady-state and time-resolved

Stern–Volmer studies and quantified with near unity efficiency using transient absorption spectroscopy.[166]

Selective excitation of the [Cr(bpmp)$_2$](PF$_6$)$_3$/DPA pair in deaerated acidified dimethylformamide (DMF) by a 532 nm laser gives blue fluorescence centered at 432 nm from DPA. The upconversion pair was quantified with a high upconversion quantum yield (Φ_{UC}) of 12% (relative to a theoretical limit of 50%[54]) (Fig. 2a and Table 2), together with an upconversion luminescence lifetime of 162 μs.[166] Excitation power density dependence study showed a moderate threshold I_{th} value of 1.56 W cm^{-2}, which is attributed to the weak absorption of the Cr(III) complex at the excitation wavelength.[166] Sterically less hindered anthracenes are known to form a dimer from the singlet excited state.[191,192] Using anthracene as the annihilator, [4+4] cycloaddition of anthracene was achieved via sTTA-UC with [Cr(bpmp)$_2$](PF$_6$)$_3$ and green light (Fig. 2d).[166] This study provides the proof-of-principle example of using a Cr(III)-based spin–flip emitter for sTTA-UC and UC-driving photocatalysis.

We recently reported another sTTA-UC example utilizing a novel dinuclear Cr(III) complex ([Cr$_2$(dNinp)$_2$(μ-OH)$_2$(μ-O$_2$CMe)]-(OTf)$_3$) (dNinp = 2,6-di(N-7-azaindol-1-yl)pyridine) as the photosensitizer.[112,193] Bridged by two hydroxo- and one carboxylato groups, the ferromagnetically coupled Cr(III) dimer with two dNinp ligands exhibits room temperature phosphorescence maximized at 728 nm with a lifetime of ∼450 ns in acetonitrile (Fig. 3 and Table 1).[112] With 9,10-bis((triisopropylsilyl)ethynyl)anthracene
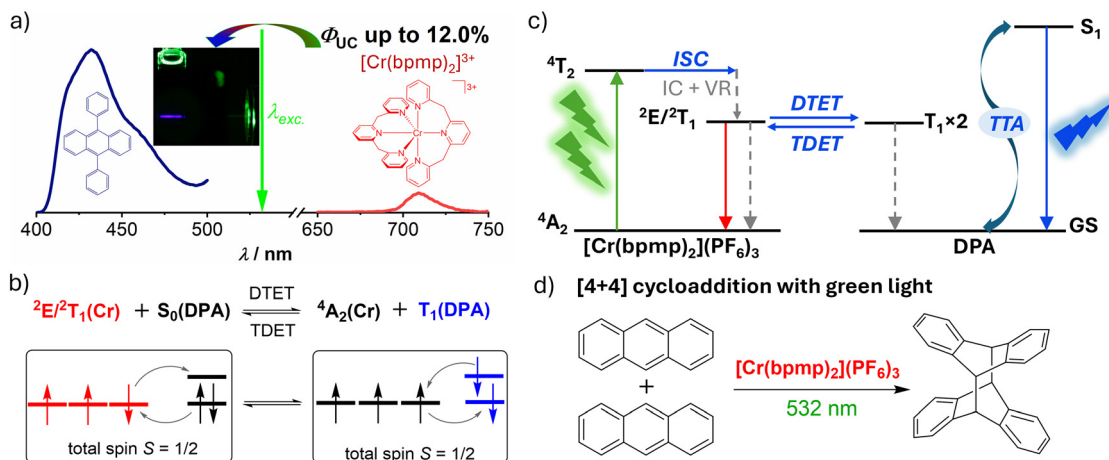
13796 | *Phys. Chem. Chem. Phys.*, 2025, **27**, 13793–13811

This journal is © the Owner Societies 2025

Fig. 2 Green-to-blue upconversion sensitized by a 3d³ Cr(III) complex. (a) Photon upconversion luminescence spectrum of the [Cr(bpmp)₂](PF₆)₃/DPA pair under 532 nm laser excitation and their molecular structures. Inset: Image of the [Cr(bpmp)₂](PF₆)₃/DPA pair under green light irradiation. (b) Reaction scheme of the excited states of [Cr(bpmp)₂]³⁺ with the ground state DPA (DTET) and the reverse process TDET, accompanied with their relevant microstates. (c) Energy level diagram of sTTA-UC for the [Cr(bpmp)₂](PF₆)₃/DPA pair. ISC: intersystem crossing, IC: internal conversion, VR: vibrational relaxation, DTET: doublet–triplet energy transfer, TDET: triplet–doublet energy transfer, TTA: triplet–triplet annihilation. (d) [4+4] cycloaddition of anthracene catalyzed by [Cr(bpmp)₂](PF₆)₃ via sTTA-UC.[166] Reproduced under terms of the CC-BY license from ref. 166. Copyright 2022, Wiley-VCH.
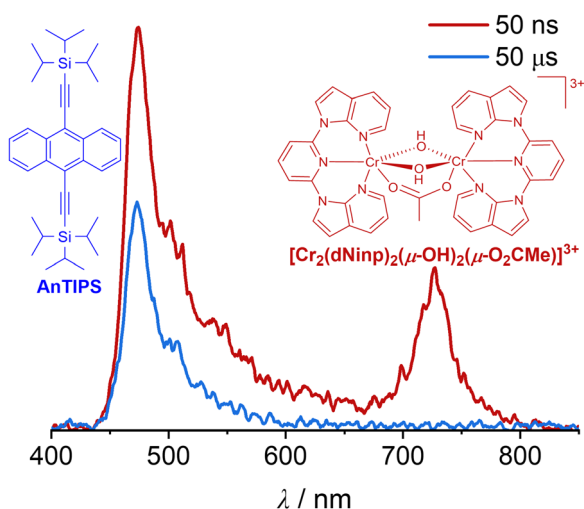
Fig. 3 Photon upconversion luminescence spectra of the Cr(III) dimer/AnTIPS pair in deaerated acetonitrile/toluene (1:1) at 20 °C with 50 ns (red traces) and 50 μs (blue traces) time delays after excitation at 532 nm (pulse energy of ~50 mJ), together with the molecular structures of the upconversion pair.[112] Reproduced under terms of the CC-BY license from ref. 112. Copyright 2024, Wiley-VCH.

(AnTIPS), a well-known blue-emissive annihilator,[26,194] DTET from the emissive spin–flip excited states of the Cr(III) dimer to the T_1 state of AnTIPS occurs upon selective excitation of the complex at 532 nm, which leads to green-to-blue upconversion with delayed fluorescence (Fig. 3).[112] Although the weak photon upconversion makes the quantitative analysis challenging, our proof-of-principle study demonstrates that luminescent Cr(III) dimers are amenable to photon upconversion and energy transfer-based applications.

For sTTA-UC sensitized by Cr(III)-based spin–flip emitters, nearly unity DTET can be achieved with the extremely long

excited state lifetime of the Cr(III) complexes, which leads to high upconversion efficiency.[166] These sTTA-UC systems are however restricted to small pseudo anti-Stokes shifts, due to the large energy gap between the absorption and the phosphorescence bands of the Cr(III)-based photosensitizers. In contrast to the strong MLCT absorption available in platinum group metal complexes, the weak metal-centered (MC) transitions of Cr(III) complexes account primarily for the comparatively high excitation power density threshold value.

3d⁵ Fe(III) complexes

Photosensitizers based on iron could be highly attractive for sTTA-UC, due to their high natural abundance, low cost, and low-energy visible light absorption. However, this still remains a significant challenge due to the extremely short excited state lifetimes for, *e.g.* 3d⁶ Fe(II) and 3d⁵ Fe(III) complexes, as a consequence of the excited state deactivation by the energetically low-lying MC states.[125,165,195–197]

Over the past few years, important processes have been achieved with 3d⁵ low-spin Fe(III) complexes bearing N-heterocyclic carbenes ligands, which show photoluminescence from the doublet ligand-to-metal charge transfer (²LMCT) excited state with a time constant up to multiple nanoseconds.[31,120,122,124,130,198] The strong σ-donating character of the carbenes destabilizes the e_g orbital and consequently the MC state,[199] leading to substantially improved photophysical properties of these Fe(III) complexes,[31,120,122,124,198] and their investigations in photoredox catalysis are gaining substantial interest.[31,124,129,200–206]

Among the luminescent Fe(III) complexes, [Fe(ImP)₂]⁺ (HImP = 1,1′-(1,3-phenylene)bis(3-methyl-1-imidazol-2-ylidene)) exhibits room temperature luminescence centered at 735 nm from the ²LMCT excited state with a lifetime of 240 ps.[122] Decoration of this complex with the different chemical

This journal is © the Owner Societies 2025

Phys. Chem. Chem. Phys., 2025, **27**, 13793–13811 | **13797**

substituents and improved synthesis[207] led to $[Fe(ImPP)_2]^+$ and $[Fe(ImPAr_2)_2]^+$ with recognized changes in the ^{2}LMCT excited state properties, including the excited state energies and lifetimes (Table 1), which allow oxidative and reductive photoredox catalysis.[31] By covalently linking multiple anthracene-based chromophores to the *meta*-positions of the outer phenyl group in $[Fe(ImPP)_2]^+$ (Fig. 4a), the lifetime of the ^{2}LMCT excited state is extended by 350 fold up to ~ 100 ns for $[Fe(CNAnt_2)_2]^+$, due to the established doublet-triplet energy reservoir between the excited states of the Fe(III) center and the anthracene moieties (Table 1).[130]

Both $[Fe(ImPP)_2]^+$ and $[Fe(CNAnt_2)_2]^+$ permit red-to-green upconversion with 9,10-bis(phenylethynyl)anthracene (BPEA) *via* an underexplored DTET from the ^{2}LMCT excited state of the Fe(III) complex to the T_1 state of BPEA (Fig. 4b).[31] Selective excitation of the $[Fe(ImPP)_2]^+$/BPEA and the $[Fe(CNAnt_2)_2]^+$/BPEA pairs with a 635 nm CW-laser leads to green fluorescence from BPEA maximized at 508 nm (Fig. 4c), which shows a delayed nature with microsecond lifetimes.[31,130] This corresponds

to a pseudo anti-Stokes shift of 0.52 eV. For the $[Fe(CNAnt_2)_2]^+$/BPEA pair, the maximal achievable Φ_{UC} is determined to be 1.30% (theoretical limit set to 50%[54]) and the I_{th} is found at ~ 1.4 W cm^{-2} under their conditions (Fig. 4d, e and Table 2).[130] These upconversion performance parameters (Φ_{UC}, I_{th}) are more than one order of magnitude improved in comparison with $[Fe(ImPP)_2]^+$ under identical conditions (Φ_{UC} = 0.019%, I_{th} = 46 W cm^{-2}).[31,130] These significantly enhanced upconversion performances are predominantly attributed to the much longer ^{2}LMCT excited state lifetime for $[Fe(CNAnt_2)_2]^+$ than $[Fe(ImPP)_2]^+$, which increases the DTET efficiency to 94% for $[Fe(CNAnt_2)_2]^+$ assuming the bimolecular quenching at the diffusion limit of 1,2-DCE at 20 °C (Table 2).[31,130] These studies provide the very few examples of utilizing Fe(III) complexes as photosensitizers for sTTA-UC, which paves the way of using Fe(III) complexes for energy transfer-based applications.

$[Fe(phtmeimb)_2]^+$ is a well-known 3d^5 Fe(III) complex with a photoluminescence quantum yield of 2.1% and a lifetime of ~ 2.0 ns from the ^{2}LMCT excited state in acetonitrile at
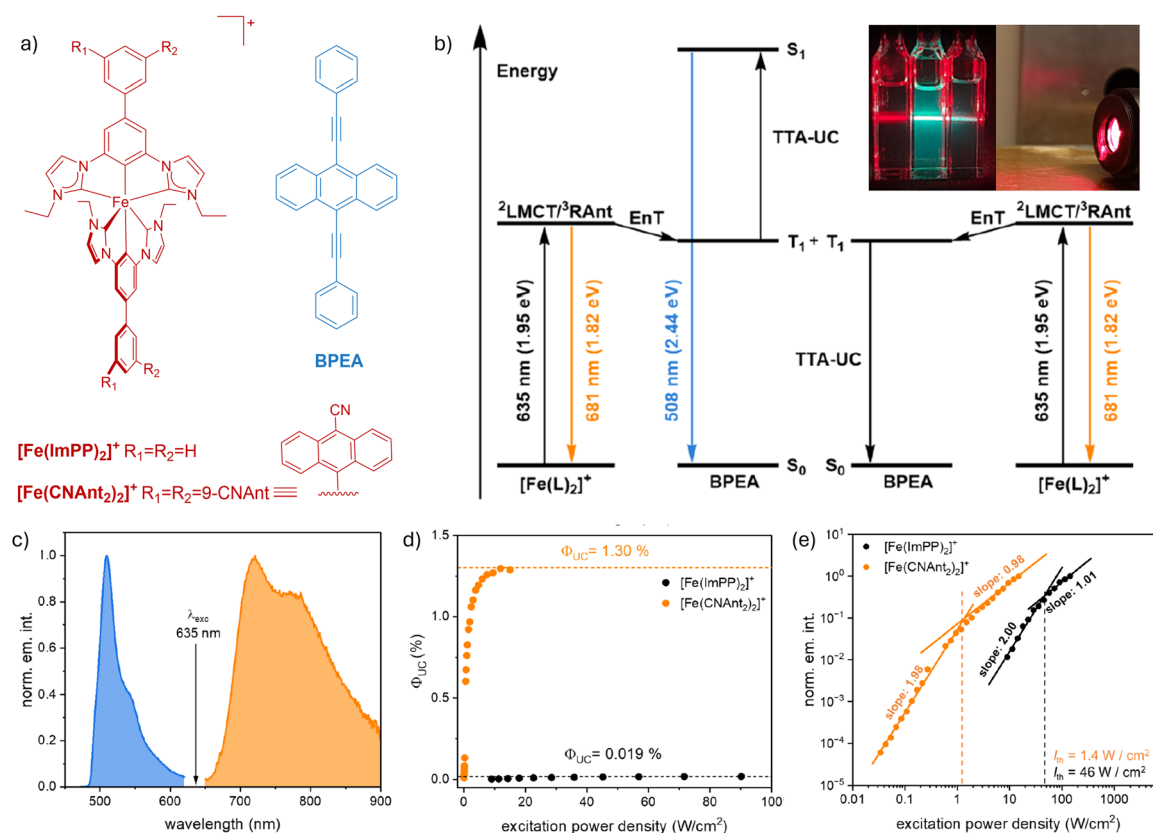

Fig. 4 Red-to-green upconversion sensitized by $[Fe(ImPP)_2]^+$ and $[Fe(CNAnt_2)_2]^+$ with 9,10-bis(phenylethynyl)anthracene (BPEA) as the annihilator. (a) Molecular structures of $[Fe(ImPP)_2]^+$, $[Fe(CNAnt_2)_2]^+$ and BPEA. (b) Energy-level diagram of sTTA-UC with $[Fe(ImPP)_2]^+$ and $[Fe(CNAnt_2)_2]^+$ as the photosensitizers and BPEA as the annihilator. Inset: Photographs of the samples containing only $[Fe(CNAnt_2)_2]^+$ without BPEA (left) and the upconverting pairs $[Fe(CNAnt_2)_2]^+$/BPEA (middle) as well as $[Fe(ImPP)_2]^+$/BPEA (right) under 635 nm CW-laser excitation (laser power = 1.0 W). (c) Normalized luminescence spectra recorded from a $[Fe(CNAnt_2)_2]^+$ solution (orange) and a solution containing the $[Fe(CNAnt_2)_2]^+$/BPEA pair (blue) in deaerated 1,2-dichloroethane at 20 °C following CW-laser excitation at 635 nm. (d) Upconversion luminescence quantum yield Φ_{UC} obtained from the upconversion pairs $[Fe(CNAnt_2)_2]^+$/BPEA (orange) and $[Fe(ImPP)_2]^+$/BPEA (black) as a function of the excitation power density at 635 nm. (e) Log–log plots of the upconversion luminescence intensity as a function of the excitation power density, giving a threshold I_{th} value of ~ 1.4 W cm^{-2} for the $[Fe(CNAnt_2)_2]^+$/BPEA pair (orange) and ~ 46 W cm^{-2} for the $[Fe(ImPP)_2]^+$/BPEA pair (black).[31,130] (b)–(e) Reproduced under terms of the CC-BY-NC-ND license from ref. 166. Copyright 2025, American Chemical Society.

13798 | *Phys. Chem. Chem. Phys.*, 2025, **27**, 13793–13811

This journal is © the Owner Societies 2025

room temperature (Table 1), which enables symmetry-breaking charge separation and photoredox catalysis.[120,200,201,203–206,208,209] In a recent study, two anthracene chromophores were covalently attached to the ligands of [Fe(phtmeimb)$_2$]$^+$, giving a Fe(III) dyad complex with μs-scaled lifetime from the dark T_1 state of the anthracenes.[129] This leads to a ten-fold enhancement of the cage escape quantum yield for the dyad with respect to the parent Fe(III) complex.[129]

Recently, we used [Fe(phtmeimb)$_2$]$^+$ as the photosensitizer and DPA annihilator for sTTA-UC (Fig. 5a). With a ^{2}LMCT excited state energy of 2.13 eV,[120] DTET from the ^{2}LMCT state of [Fe(phtmeimb)$_2$]$^+$ to the T_1 state of DPA is thermodynamically feasible with a large driving force of ~ 0.4 eV (Fig. 5b),[166,210] inhibiting the reversed process. Steady-state luminescence study, time-resolved transient absorption study, and NMR titration synergistically found that [Fe(phtmeimb)$_2$]$^+$ and DPA are
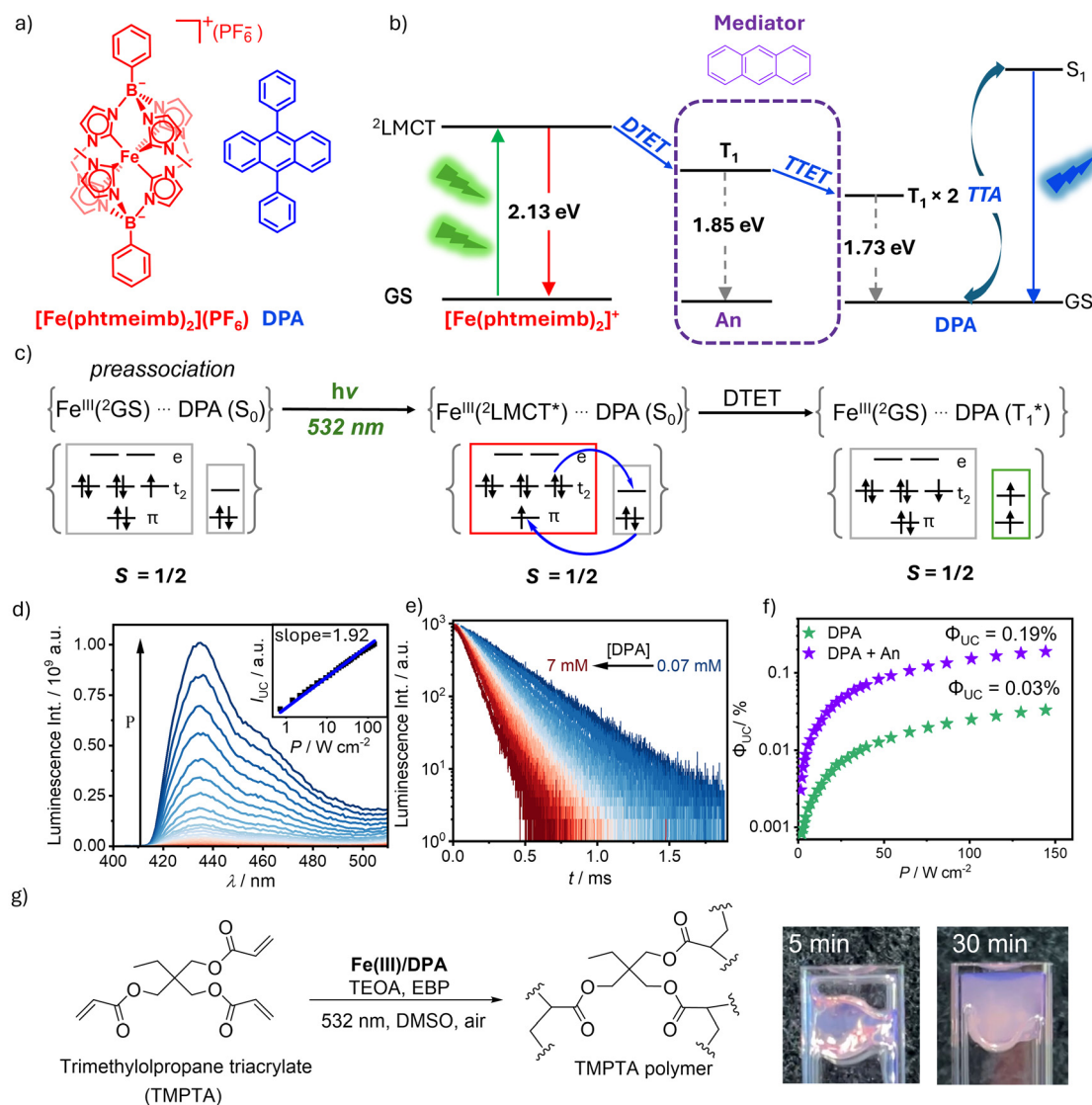

Fig. 5 Green-to-blue upconversion and photopolymerization sensitized by [Fe(phtmeimb)$_2$](PF$_6$) with 9,10-diphenylanthracene (DPA) as the annihilator.[36] (a) Molecular structures of [Fe(phtmeimb)$_2$](PF$_6$) and DPA. (b) Energy-level diagram of sTTA-UC with the [Fe(phtmeimb)$_2$](PF$_6$)/DPA pair with anthracene (An) as a mediator. DTET: doublet–triplet energy transfer; TTET: triplet–triplet energy transfer; and TTA: triplet–triplet annihilation. (c) Reaction scheme of DTET for the [Fe(phtmeimb)$_2$](PF$_6$)/DPA pair with their corresponding electronic microstates. (d) Upconversion luminescence spectra of [Fe(phtmeimb)$_2$](PF$_6$) (40 μM)/DPA (10 mM) in aerated DMSO at 20 °C, excited with a green 532 nm CW-laser at different powers (1 to 200 mW). Inset: Excitation power density dependence of the upconversion luminescence integral from 410 to 510 nm as a log–log plot. (e) Normalized upconversion luminescence decay at 430 nm recorded from solutions containing [Fe(phtmeimb)$_2$](PF$_6$) (40 μM) with different concentrations of DPA (0.07–7 mM) in aerated DMSO at 20 °C. Excitation occurred with the 532 nm laser (200 mW) with a pulse width of 250 μs. (f) Upconversion luminescence quantum yield (Φ_{UC}) of the [Fe(phtmeimb)$_2$](PF$_6$) (40 μM)/DPA (10 mM) pair in the absence and presence of An (10 mM) as the mediator in aerated DMSO at 20 °C as a function of the excitation power density (532 nm CW-laser).[36] (g) Photopolymerization reaction scheme of trimethylolpropane triacrylate (TMPTA) with its respective polymerization images at the indicated irradiation time with a 532 nm CW-laser.[36] Reproduced under terms of the CC-BY license from ref. 36. Copyright 2024, American Chemical Society.

This journal is © the Owner Societies 2025

Phys. Chem. Chem. Phys., 2025, **27**, 13793–13811 | **13799**

preassociated in their ground states via π–π stacking, which is beneficial for distance-dependent Dexter-type energy transfer with a short-lived ^{2}LMCT excited state.[36] This leads to enhanced DTET with an efficiency of 22.5%, which exceeds the estimated DTET efficiency (~9.6%) at the diffusion limit of DMSO at 20 °C.[36] Notably, this DTET differs from that for the above-mentioned 3d^3 Cr(III) complexes and anthracenes, because the spin of the Fe(III) complex remains unchanged, whereas the spin of DPA changes from singlet to triplet during DTET (Fig. 5c).[36] Despite this unusual behavior, the DTET for the [Fe(phtmeimb)$_2$]$^+$/DPA pair is a spin-allowed process with conserved total spin according to the Wigner spin rule (Fig. 5c).[189,190,211]

Selective excitation of the [Fe(phtmeimb)$_2$]$^+$/DPA pair with a 532 nm CW-laser in aerated DMSO leads to upconverted blue emission from the S$_1$ state of DPA maximized at 435 nm, giving a pseudo anti-Stokes shift ΔE of 0.52 eV (Fig. 5c).[36] The integrated upconversion luminescence $I_{410–510}$ displays a quadratic dependence on the excitation power density (slope of 1.92), indicating the biphotonic nature of TTA (second-order reaction) (Fig. 5d).[59] The upconversion luminescence lifetime τ_{UC} shows a delayed nature, which ranges from 304 to 110 μs with increasing DPA concentration, due to the more frequent encounters among the T$_1$-excited DPA (Fig. 5e). The reachable upconversion quantum yield Φ_{UC} was determined to be 0.03% (relative to a theoretical limit of 50%)[54] for the [Fe(phtmeimb)$_2$]$^+$/DPA pair, which can be enhanced by a factor of six to 0.19% by adding anthracene (An) as a triplet mediator (Fig. 5b, f and Table 2).[36]

We employed the Fe(III)/DPA upconversion pair to drive the catalytic polymerization of acrylate monomers like trimethylol-propane triacrylate (TMPTA) with low-energy green light (Fig. 5g).[36] The S$_1$-excited DPA accessed via sTTA-UC is reductively quenched by triethanolamine (TEOA), giving a strongly reducing DPA radical anion that acts as the initiator for radical polymerization (Fig. 5g).[36] However, photoinduced electron transfer with TEOA is kinetically hindered for prompt DPA, due to the substantially shorter lifetime. This study provides a new strategy for photopolymerization by leveraging low-energy light, long upconversion luminescence lifetime, and the photoredox properties of sTTA-UC.

3d^6 Cr(0) complexes

In recent years, significant progress has been made with photoactive coordination compounds with a 3d^6 valence electronic configuration including Cr(0),[29,111,127,162,167,212–214] Mn(I),[116,117,214,215] Fe(II),[117,121,123,125,126,128] and Co(III) complexes.[131–133] Differing from the 4d^6 and 5d^6 electronic configurations based on platinum group metals, complexes with 3d^6 configurations have fundamentally different excited state electronic structures.[216] Important understandings of these novel first-row transition metal complexes have been gained, and their promising excited state properties make them emerging photocatalysts.[125,126,134,165,217] However, only extremely few examples have employed these complexes for sTTA-UC,[27,116,167] mainly due to their very short excited state lifetimes caused by the deactivation from the MC states.

The first attempt of using a photoactive 3d^6 metal complex for sTTA-UC was made with a Cr(0) complex with chelating diisocyanide ligands (Cr(CN^{t}BuAr$_3$NC)$_3$) as the photosensitizer and anthracene annihilator in deaerated toluene (Fig. 6a).[167] Upon excitation of the MLCT absorption centered at ~500 nm, the Cr(0) complex shows luminescence maximized at 630 nm from the ^{3}MLCT excited state with time constants of 0.64 ns (83%) and 4.33 ns (17%) in toluene at 20 °C (Fig. 6b and Table 1). Despite these short ^{3}MLCT excited state lifetimes, TTET to the T$_1$ state of anthracene (10 mM) occurs, as evidenced by transient absorption signatures of the triplet anthracene with a time constant of ~170 μs (Fig. 6c and d).[167]

For the Cr(CN^{t}BuAr$_3$NC)$_3$/anthracene pair, selective excitation at 530 nm leads to purple fluorescence from anthracene maximized at 405 nm, which decays with a time constant of ~65 μs (Fig. 6e and f).[167] This gives a pseudo anti-Stokes shift of 0.72 eV. The upconversion luminescence exhibits a nonlinear dependence on the excitation power, due to the biphotonic upconversion process.[57,59] Notably, the transient absorption study of the upconversion pair reveals a bleaching of the ^{1}MLCT absorption of the Cr(0) complex, which recovers with a time constant of ~30 μs, predominantly due to the Förster-type energy transfer from the upconverted S$_1$ state of anthracene to the ^{1}MLCT state of the Cr(0) complex.[167] This proof-of-principle study of using the Cr(0) complex for sTTA-UC promises the potential of using photoactive 3d^6 metal complexes for applications based on energy transfer and photon upconversion.

A recent report of a pyrene-decorated Cr(0) isocyanide complex Cr(L^{pyr})$_3$ (Fig. 7a) shows a luminescent ^{3}MLCT excited state centered at 740 nm with a lifetime of 24 ns in deaerated toluene at 20 °C (Table 1).[29] Using AnTIPS (5 mM) as the annihilator, TTET from the ^{3}MLCT excited state of Cr(L^{pyr})$_3$ to the T$_1$ state of AnTIPS occurs, as evidenced with the finger-like transient absorption spectral features of AnTIPS with a decay time constant of 140 μs (Fig. 7b).[27] The TTET efficiency was determined to be 40% for the Cr(L^{pyr})$_3$ (20 μM)/AnTIPS (5 mM) pair in deaerated toluene at 20 °C, which is mainly restricted by the relatively short lifetime of the photosensitizer.

Selective excitation of the Cr(L^{pyr})$_3$/AnTIPS pair at 705 nm yields blue fluorescence from AnTIPS maximized at 470 nm, corresponding to a large pseudo anti-Stokes shift of 0.88 eV.[27] The upconversion luminescence decays with a time constant of 72 μs (Fig. 7c), which accounts for roughly half of the observed triplet lifetime of AnTIPS (Fig. 7b), in line with literature reports.[28,35,58] Excitation power density dependent study of the upconversion luminescence shows a quadratic to linear dependence with a threshold I_{th} found at 5.9 W cm^{-2}, above which the upconversion reaches saturation (Fig. 7d).[59] In comparison to the red-to-blue sTTA-UC sensitized by Os(II) or Pt(II) complexes, in which the I_{th} values are often below 1 W cm^{-2} in solution,[51,72,82,83] the relatively high I_{th} for the Cr(L^{pyr})$_3$/AnTIPS pair is attributed to the significantly short ^{3}MLCT lifetime and the weak absorption at the irradiation wavelength.[55,57] The maximal achievable Φ_{UC} was determined to be ~2% for the Cr(L^{pyr})$_3$/AnTIPS pair under the chosen conditions (Fig. 7e and Table 2).[27] This is a competitive value

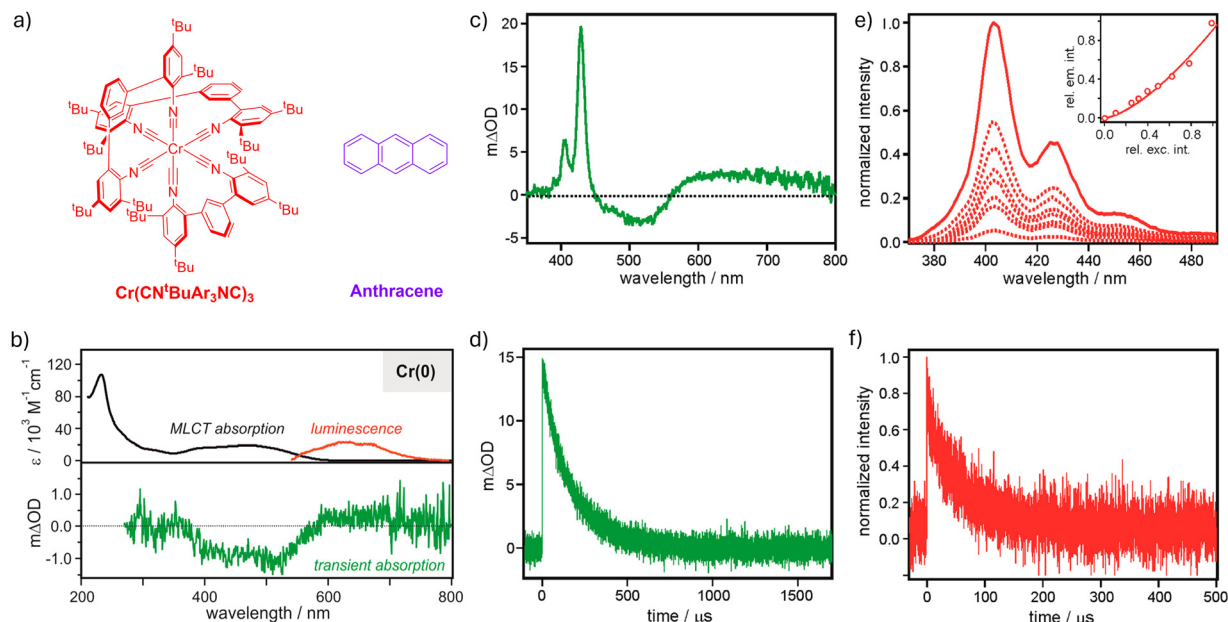**13800** | Phys. Chem. Chem. Phys., 2025, **27**, 13793–13811

This journal is © the Owner Societies 2025

Fig. 6 Green-to-purple upconversion sensitized by $Cr(CN^tBuAr_3NC)_3$ with an anthracene annihilator. (a) Molecular structures of $Cr(CN^tBuAr_3NC)_3$ and anthracene. (b) UV-vis absorption (black trace) and luminescence (red) spectra (upper panel) and UV-vis transient absorption spectrum (green, bottom panel) of $Cr(CN^tBuAr_3NC)_3$ in deaerated THF at 20 °C. Excitation at 450 nm was used for the luminescence measurement and at 532 nm with a ps-pulsed laser for the transient absorption measurement. (c) Transient absorption spectrum of the $Cr(CN^tBuAr_3NC)_3$ (20 μM)/anthracene (10 mM) pair in deaerated toluene at 20 °C, and (d) the decay kinetics of the transient absorption signal at 430 nm. Excitation occurred at 532 nm with a ns-pulsed laser. (e) Upconversion luminescence spectra of the sample from (c) at different excitation power densities at 530 nm and the dependence of the relative upconversion luminescence intensity at 405 nm on the relative excitation intensity at 530 nm (inset), and (f) upconversion luminescence decay of the sample from (c) at 403 nm under 532 nm excitation.[167] Reproduced with permission from ref. 167. Copyright 2017, American Chemical Society.

for red-to-blue upconversion, even in comparison with photosensitizers based on Os(II) complexes.[47,50,51,82,83,218,219] In particular, the $Cr(L^{pyr})_3$/AnTIPS pair exhibits remarkable photostability under continuous laser irradiation at a high power density (18.6 W cm^{-2}). The high photorobustness of the upconversion luminescence makes it suitable as a blue lamp for initiating the radical polymerization of acrylamide in an aqueous solution with 705 nm irradiation, yielding a free-standing hydrogel of polyacrylamide (Fig. 7f).[27] This expands the very few examples of red light induced polymerization via sTTA-UC.[220–222]

3d^6 Mn(I) complexes

Recent breakthroughs with coordination compounds based on 3d^6 metals have led to a few photoactive Mn(I) complexes,[116,117,223,224] among which two Mn(I) complexes with chelating isocyanide ligands are amenable to sensitizing photon upconversion.[116] The Mn(I) complex with tridentate isocyanide ligands (Fig. 8a) exhibits luminescence from the MLCT excited state (2.9 eV) with an average lifetime of 1.73 ns in deaerated acetonitrile at 20 °C and shows a ligand-centered $^3\pi$–π^* state at ~2.3 eV that becomes emissive at low temperature (Fig. 8b and Table 1).[116]

The long-lived triplet state of anthracene is sensitized by $[Mn(L^{tri})_2]^+$ via TTET, as evidenced by the characteristic transient absorption signatures of triplet anthracene upon selective excitation of the Mn(I) complex at 420 nm.[116] The TTET efficiency was determined with relative actinometry experiments to 12.1% under optimized conditions (Table 2). Notably, the TTET

occurs from the $^3\pi$–π^* excited state to anthracene instead of from the emissive MLCT state, despite the larger driving force for the latter (Fig. 8b). Likely, the emissive MLCT state has a substantial singlet character, which makes the energy transfer to triplet anthracene a spin-forbidden process. Nevertheless, upconversion luminescence from anthracene was observed for the $[Mn(L^{tri})_2]^+$ (25 μM)/anthracene (40 μM) pair with selective excitation at 420 nm, and no fluorescence was detected in the absence of the Mn(I) complex under identical conditions.[116] Analogue energy transfer and sTTA-UC studies were made with another Mn(I) complex with bidentate isocyanide ligands.[116] These proof-of-concept studies open the door to using photoactive Mn(I) for sTTA-UC.

3d^{10} Cu(I) complexes

Photoactive Cu(I) coordination compounds have been extensively explored for decades,[142–149,225,226] primarily because the completely filled 3d^{10} subshell excludes the energetically low-lying MC states that often depopulate the charge transfer (CT) excited states significantly.[163,227,228] Recent advances with Cu(I) bis-1,10-phenanthroline complexes provide important guidelines for stabilizing the ^{3}MLCT excited states, leading to a series of Cu(I) complexes with long lifetimes.[146,147,149,164,229]

Among the phenanthroline-based Cu(I) complexes, $[Cu(dsbtmp)_2](PF_6)$ (dsbtmp = 2,9-di(sec-butyl)-3,4,7,8-tetramethyl-1,10-phenanthroline) (Fig. 9a) exhibits bright luminescence at ~630 nm with an impressively long lifetime (τ = 1.2–2.8 μs) from the ^{3}MLCT excited state (Table 1), due to the suppressed
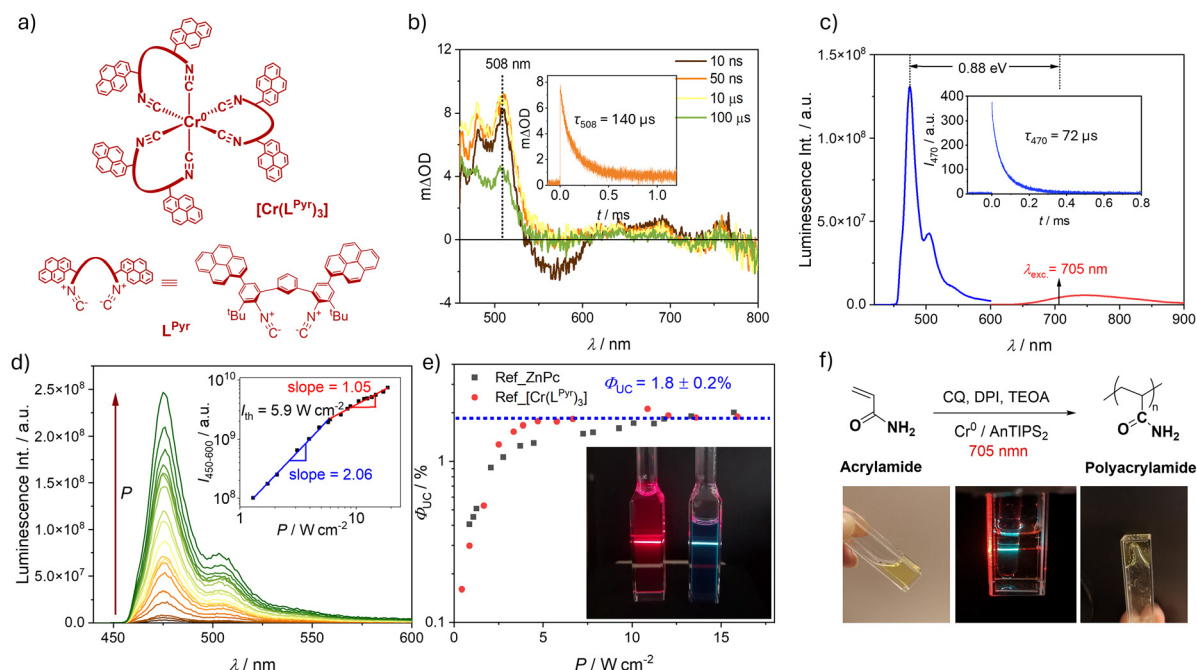
This journal is © the Owner Societies 2025

Phys. Chem. Chem. Phys., 2025, 27, 13793–13811 | 13801

Fig. 7 Red-to-blue upconversion sensitized by $Cr(L^{pyr})_3$ with AnTIPS annihilator.[27] (a) Molecular structures of $Cr(L^{pyr})_3$. (b) Transient absorption spectra of the $[Cr(L^{pyr})_3]$ (20 μM)/AnTIPS (5 mM) pair recorded after different time delays in deaerated toluene at 20 °C. Inset: Transient absorption decay of the upconversion pair recorded at 508 nm under 532 nm excitation. (c) Upconversion luminescence spectrum of the sample from (b) at 20 °C under 705 nm CW-laser excitation (45 mW) (blue trace) and the prompt emission of $[Cr(L^{pyr})_3]$ (20 μM) under 550 nm excitation (red trace). Inset: Decay kinetics of the upconversion luminescence at 470 nm under 532 nm ns-pulsed laser excitation. (d) Excitation power density dependent upconversion luminescence spectra of the sample from (b) at 20 °C and inset: The derived log−log plot of the integrated upconversion luminescence as a function of the excitation power density. Excitation occurred with a 705 nm CW-laser with various power densities (*P*) (1.3 to 18.6 W cm^{-2}). (e) Φ_{UC} of the upconversion pair from (b) at 20 °C as a function of the excitation power density (705 nm CW-laser), determined independently with two different references, ZnPc (1 μM) and $[Cr(L^{pyr})_3]$ (20 μM), respectively. Inset: Photograph of the employed reference ZnPc solution (left) and the upconversion pair (right) under 705 nm laser irradiation. (f) Reaction scheme of the photopolymerization of acrylamide using the $[Cr(L^{pyr})_3]$/AnTIPS upconversion pair at 705 nm irradiation, and photographs of the aqueous reaction mixture for polymerization before (left), during (middle), and after (right) the 705 nm laser irradiation for several hours. CQ: camphorquinone; TEOA: triethanolamine; DPI: diphenyliodonium chloride.[27] Reproduced under terms of the CC-BY-NC-ND license from ref. 27. Copyright 2023, Wiley-VCH.
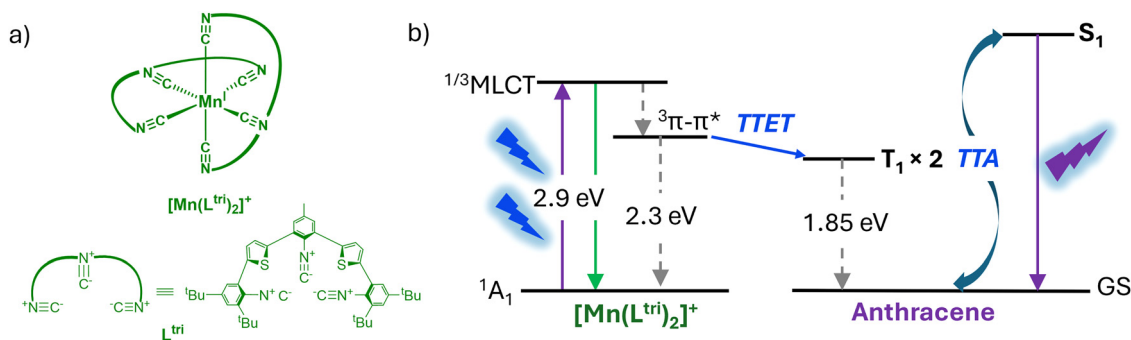

Fig. 8 Blue-to-purple upconversion sensitized by $[Mn(L^{tri})_2]^+$ with an anthracene annihilator. (a) Molecular structure of $[Mn(L^{tri})_2]^+$. (b) Energy level diagram illustrating sTTA-UC sensitized by $[Mn(L^{tri})_2]^+$. TTET: triplet−triplet energy transfer, TTA: triplet−triplet annihilation.

ground- and excited-state distortion achieved with cooperative steric effects.[230] This long lifetime leads to high TTET efficiencies of >90% with millimolar concentrations of the annihilators, *i.e.*, anthracene (An), 9,10-dimethylanthracene (DMA), or DPA (Fig. 9a).[141] In the presence of the anthracene derivatives, selective excitation of $[Cu(dsbtmp)_2](PF_6)$ at 488 nm leads to near-UV fluorescence from the anthracenes, which follows

quadratic to linear dependence on the excitation power density in deaerated dichloromethane at room temperature (Fig. 9b and c). This gives I_{th} values of near 1 W cm^{-2} for the investigated $[Cu(dsbtmp)_2](PF_6)$ (0.78 mM)/anthracene pairs (Fig. 9c). These I_{th} values, which can be tuned by monitoring the absorbance of the photosensitizer,[55,231] are above the solar irradiance at this excitation wavelength, but remain lower
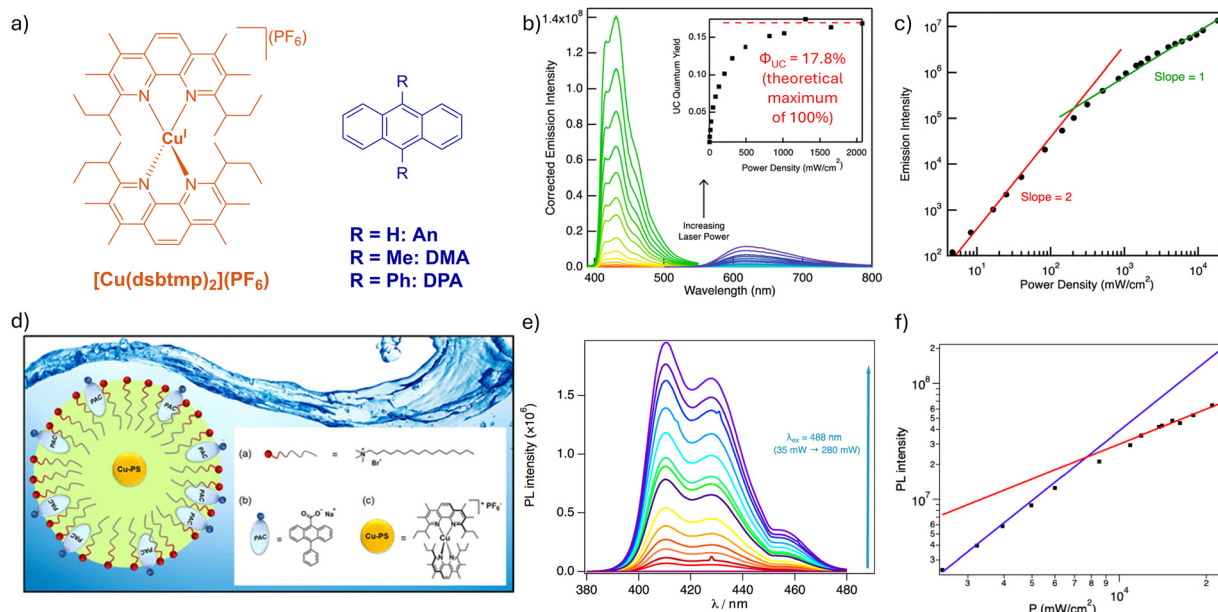
13802 | *Phys. Chem. Chem. Phys.*, 2025, **27**, 13793–13811

This journal is © the Owner Societies 2025

Fig. 9 Cyan-to-blue/purple upconversion sensitized by [Cu(dsbtmp)$_2$](PF$_6$) with anthracene derivatives as the annihilator. (a) Molecular structures of [Cu(dsbtmp)$_2$](PF$_6$) and the employed anthracenes. (b) Luminescence spectra of the [Cu(dsbtmp)$_2$](PF$_6$) (0.12 mM)/DPA (8.9 mM) pair in deaerated dichloromethane (green to orange traces) and the luminescence spectra of a [Ru(bpy)$_3$](PF$_6$)$_2$ reference solution in acetonitrile (purple to blue traces) under various excitation powers at 488 nm. Inset: Upconversion quantum yield Φ_{UC} plotted as a function of the excitation power density P.[141] (c) Double logarithmic plot of the upconversion luminescence monitored at 385 nm for An as a function of the excitation power density at 488 nm obtained for the [Cu(dsbtmp)$_2$](PF$_6$) (0.76 mM)/An (5 mM) pair. (b) and (c) Reproduced with permission from ref. 141. Copyright 2015, American Chemical Society. (d) Schematic illustration of photon upconversion micelles made of cetyltrimethylammonium bromide surfactant and the [Cu(dsbtmp)$_2$](PF$_6$)/PAC (10-phenylanthracene-9-carboxylate) upconversion pair in water, together with their molecular structures. (e) Excitation power density-dependent upconversion luminescence spectra of the Cu-PS-PAC assembly from (d) at 488 nm excitation and (f) their corresponding double logarithmic plot.[144] (d)–(f) Reproduced with permission from ref. 144. Copyright 2020, American Chemical Society.

than many sTTA-UC sensitized by earth-abundant metal complexes.[27,31,166] For the [Cu(dsbtmp)$_2$](PF$_6$) (0.12 mM)/DPA (8.9 mM) pair in deaerated dichloromethane, a Φ_{UC} of 8.9% (theoretical maximum of 50%[54]) was reached (Fig. 9b and Table 2), which is twice higher than the Φ_{UC} obtained with DMA and roughly 10 times higher than that with An, due to the exciplex formation and the low fluorescence quantum yield of the latter.[141]

Changing the annihilator to negatively charged 10-phenyl-anthracene-9-carboxylate (PAC), the authors later immobilized the [Cu(dsbtmp)$_2$]$^+$/PAC upconversion pair to a micellar assembly made of cetyltrimethylammonium bromide surfactant (Fig. 9d).[144] The hydrophobic Cu(I) complex is encapsulated within the micelle, while the anionic PAC binds electrostatically to the cationic assembly surface. Selective excitation of the aqueous upconversion assembly at 488 nm gives the characteristic fluorescence of PAC, and the excitation power density dependence study reveals a I_{th} value of 7.7 W cm^{-2} (Fig. 9e and f). This value is substantially higher than the I_{th} values for the [Cu(dsbtmp)$_2$]$^+$/anthracene pairs in organic solvents,[141] which is likely attributed to the relatively lower TTET efficiency and the hindered TTA event in the micellar confinement.[55,231] Attempts to increase the photosensitizer concentration failed to give a lower I_{th} value, because the assembly became turbid at a high loading concentration.[144] The [Cu(dsbtmp)$_2$]$^+$/PAC upconversion assembly was further investigated for electron transfer with an electron acceptor

methyl viologen (MV^{2+}), yielding the transient absorption features of MV$^{\bullet+}$.[144] This combination of micellar architecture and photon upconversion system makes photochemistry viable in water with low irradiation energy.

3d^{10} Zn(II) complexes

Zn(II) porphyrin complexes with ligand-based photophysics have often been used as photosensitizers for sTTA-UC (Fig. 10), due to the low-energy of the Q absorption band, the relatively high intersystem crossing (ISC) efficiency,[232] and the long-lived T$_1$ dark state.[233] Using perylene derivatives as an annihilator (Fig. 10 and Table 1), several red-to-green or green-to-blue upconversion sensitized by Zn(II) complexes have been reported, which exhibit mostly relatively small pseudo anti-Stokes shifts, as shown in Table 2. Notably, the ZnTPPOH/TBPer upconversion pair shows a high Φ_{UC} of 12% at remarkably low concentrations of the TBPer annihilator (Table 2).[172] Solid-state near infrared upconversion was achieved with the F$_{16}$ZnPc/PDI-CH$_3$ pair (Fig. 10), from which one electron is injected from the upconverted S$_1$-state of PDI-CH$_3$ into TiO$_2$, and this is highly attractive for photovoltaics.[173]

Recent fundamental developments for Zn(II) complexes have received substantial attention with triplet charge-transfer states[152,234,235] or TADF characteristics.[153,236,237] Among these new types of Zn(II) complexes with long-lived triplet excited states, fluorescent [Zn(m-L)$_2$] (Fig. 10) shows a long-lived dark state from the triplet intraligand charge-transfer (^{3}ILCT)

This journal is © the Owner Societies 2025

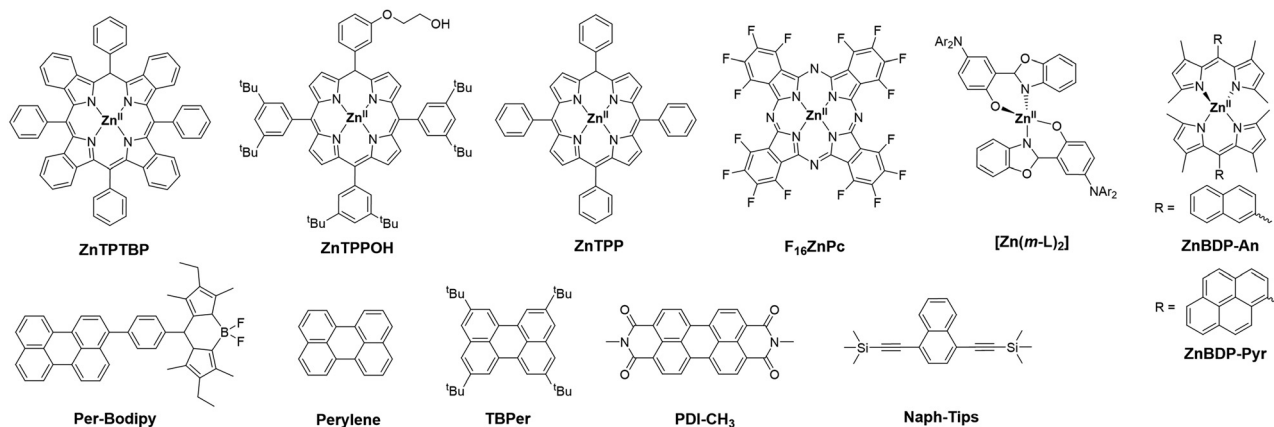*Phys. Chem. Chem. Phys.*, 2025, **27**, 13793–13811 | **13803**

Fig. 10 Molecular structures of the Zn(II)-based photosensitizers and organic annihilators used for sTTA-UC.

(Table 1). This long-lived ^{3}ILCT allows blue-to-UV upconversion with naphthalene substituted with triisopropylsilyl (Naph-Tips, Fig. 10), giving a Φ_{UC} of 0.73%.[152]

For the ZnTPP derivatives, unusual homomolecular sTTA-UC from the S$_2$ excited state has been frequently observed.[23,168,171] Selective excitation of these Zn(II) complexes at 532 nm populates the emissive S$_2$ state at ~430 nm via TTA between the two ZnTPP molecules.[23,168,171] Interestingly, the upconverted S$_2$ state of ZnTPP undergoes electron transfer to acrylate monomers, allowing direct initiation of polymerization reactions with green light.[23]

4d^0 Zr(IV)-based photosensitizer

Zirconium, as the fourth most abundant transition metal, seems attractive for developing low-cost luminophores or photosensitizers. The electron-deficient 4d^0 configuration of Zr(IV) allows coordination with electron-rich ligands, e.g. pyridinedipyrrolide (PDP), which elevate Zr(IV) complexes with long phosphorescence lifetimes from the triplet ligand-to-metal charge transfer (^{3}LMCT) state.[155,156,238] Zr(^{Mes}PDP^{Ph})$_2$ (Fig. 11a) exhibits strong photoluminescence maximized at 581 nm with a high quantum

yield (Φ_{PL}) of 45% and a long lifetime of 350 μs in solution at room temperature (Table 1).[156] This long-lived ^{3}LMCT excited state promotes near unity TTET to DPA or carbazole-based DPA derivatives (CzPA) (Fig. 11a) at a remarkably low concentration of 0.25 mM. With this annihilator concentration, only linear excitation power density dependence was observed from the upconversion luminescence for the Zr(^{Mes}PDP^{Ph})$_2$/DPA pair upon 514 nm excitation (Fig. 11b). At an excitation power density of ~13 mW cm^{-2}, which is substantially lower than the solar irradiance of 26.7 mW cm^{-2} in this absorption regime, all investigated photosensitizer/annihilator pairs reach upconversion saturation, giving high Φ_{UC} values ranging from 15.9 to 21.4% (theoretical maximum set to 50%[54]) (Fig. 11c and Table 2).[175] These high Φ_{UC} values, the low required excitation power densities, and the high abundance of zirconium make Zr(^{Mes}PDP^{Ph})$_2$ very promising for future solar energy-based applications.

4d^6 Mo(0)-based complexes

Earth-abundant Mo(0) shares the 4d^6 electronic configuration with Ru(II), which makes it an attractive substitute for the
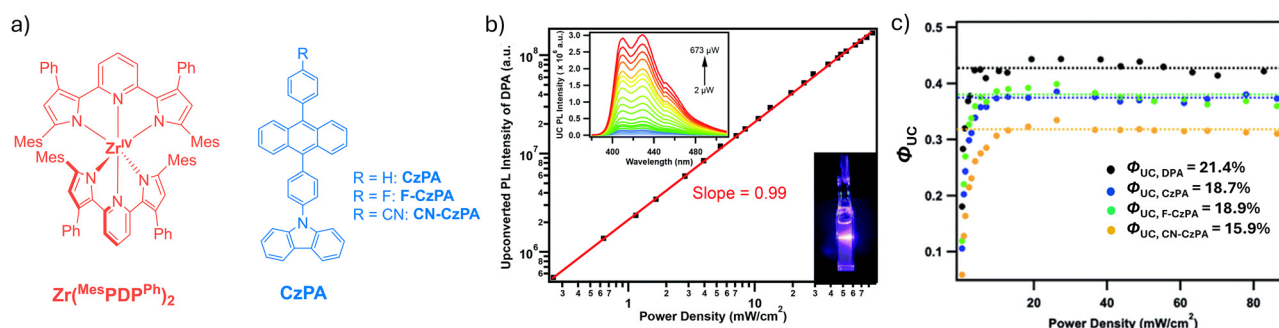

Fig. 11 Green-to-blue upconversion sensitized by Zr(^{Mes}PDP^{Ph})$_2$ with DPA and carbazole-based DPA derivatives (CzPA) as the annihilator.[175] (a) Molecular structures of Zr(^{Mes}PDP^{Ph})$_2$ and the CzPA annihilators. (b) Double logarithmic plot of integrated upconversion luminescence intensity for the Zr(^{Mes}PDP^{Ph})$_2$/DPA (0.25 mM) pair in deaerated THF as a function of the excitation power density at 514 nm, and the corresponding upconversion luminescence spectra (upper inset). Bottom inset: Image of the upconversion sample under 514 nm irradiation. (c) Upconversion quantum yields (theoretical maximum set to 50%[54]) determined with a Zr(^{Mes}PDP^{Ph})$_2$ photosensitizer and DPA or CzPAs annihilator in deaerated THF, plotted as a function of the excitation power density at 514 nm.[175] Reproduced under terms of the CC-BY license from ref. 175. Copyright 2021, Royal Society of Chemistry.
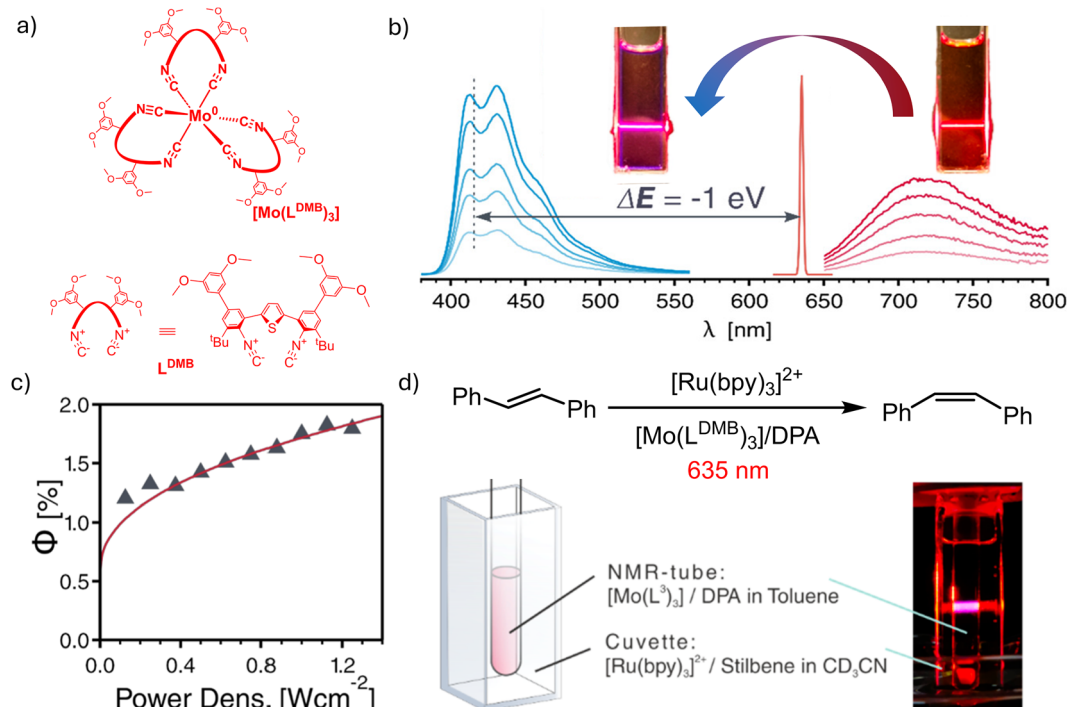
13804 | *Phys. Chem. Chem. Phys.*, 2025, **27**, 13793–13811

This journal is © the Owner Societies 2025

Fig. 12 Red-to-blue upconversion and photoisomerization sensitized by [Mo(L^{DMB})$_3$] with 9,10-diphenylanthracene (DPA) as the annihilator. (a) Molecular structures of [Mo(L^{DMB})$_3$] as the photosensitizer. (b) Luminescence spectra recorded from a [Mo(L^{DMB})$_3$] solution (red traces) and a solution containing the [Mo(L^{DMB})$_3$]/DPA pair (blue traces) in deaerated toluene at 20 °C following CW-laser excitation at 635 nm with different power densities. Inset: Photographs of the upconverting sample with the [Mo(L^{DMB})$_3$]/DPA pair (left) and the sample containing only [Mo(L^{DMB})$_3$] but no DPA (right) under 635 nm laser excitation. (c) Upconversion luminescence quantum yield Φ_{UC} obtained with [Mo(L$_3$)$_3$] (12 μM) and DPA (50 mM) (grey triangles) as a function of the excitation power density at 635 nm. (d) Photochemical isomerization reaction in separated vessels via photon upconversion with red irradiation light. A sealed NMR tube containing 13 μM [Mo(L^{DMB})$_3$] and 60 mM DPA in deaerated toluene is immersed into the cuvette containing 0.3 mM [Ru(bpy)$_3$]$^{2+}$ and 17 mM trans-stilbene in deaerated CD$_3$CN. Red-to-blue upconversion inside the NMR tube is visible by the naked eye (right).[157] Reproduced under terms of the CC-BY-NC-ND license from ref. 157. Copyright 2021, American Chemical Society.

precious metal ions.[161,162,239] The luminescent Mo(0) complex with chelating diisocyanide ligands ([Mo(L^{DMB})$_3$]) exhibits strong MLCT absorptions tailing to 550 nm and bright ^{3}MLCT luminescence at ~720 nm with an excited-state lifetime of 54 ns in toluene at 20 °C (Fig. 12a and Table 1).[157] These photophysical properties make [Mo(L^{DMB})$_3$] a suitable photosensitizer for sTTA-UC with e.g. DPA. Photoexcitation of the [Mo(L^{DMB})$_3$]/DPA pair with a CW-laser at 635 nm across various excitation power densities leads to delayed fluorescence from DPA, giving a pseudo anti-Stokes shift of 0.93 eV (Fig. 12b and Table 2).[157] The achievable Φ_{UC} for the [Mo(L^{DMB})$_3$]/DPA pair in deaerated toluene was determined to be 1.8% (theoretical maximum of 50%)[54] under optimized conditions (Fig. 12c). This Φ_{UC} value approaches that of many sTTA-UC systems with precious metal-based photosensitizers,[22] including some of the recently reported systems with a record pseudo anti-Stokes shifts of around 1 eV.[71,72,83,218,240] Based on this upconversion performance, the [Mo(L^{DMB})$_2$]/DPA pair has been used to drive a blue-light-dependent sensitized photoisomerization reaction in a two-vessel setup.[157] The upconverted blue light from the NMR tube was reabsorbed by [Ru(bpy)$_3$]$^{2+}$ (bpy = 2,2'-bipyridine) in the surrounding cuvette, which catalyzes the isomerization of trans-stilbene to cis-stilbene with a reaction yield of 50% after 17 hours of irradiation (Fig. 12d).[157]

Another sTTA-UC example sensitized by the Mo(0) complex was recently made with [Mo(CO)$_3$(tpe)] (tpe = 1,1,1-tris(pyrid-2-yl)ethane), which was prepared with a high yield over 78% following relatively simple synthetic routes (Fig. 13a).[158] This photorobust Mo(0) complex exhibits deep-red ^{3}MLCT luminescence with a lifetime of several hundred nanoseconds (Table 1).[158] This long-lived ^{3}MLCT excited state permits efficient TTET to DPA with a Φ_{TTET} of 85%,[158] which consequently leads to upconversion luminescence of DPA centered at 435 nm (Fig. 13b). Excitation power density dependent study of the upconversion luminescence reveals the quadratic to linear dependence with a low threshold I_{th} value found at 90 mW cm^{-2} and a maximal Φ_{UC} of 12% (theoretical maximum of 50%[54]) (Fig. 13c and Table 2). This study underscores the potential of tripodal ligand-based carbonyl complexes in photochemical applications, offering a pathway to bypass the use of precious metals and complex ligand synthesis.

Conclusion

Substituting precious elements in photoactive complexes with abundant transition metals remains a significant challenge in the fields of coordination chemistry and photochemistry. Unlike the luminescent platinum group metal complexes with
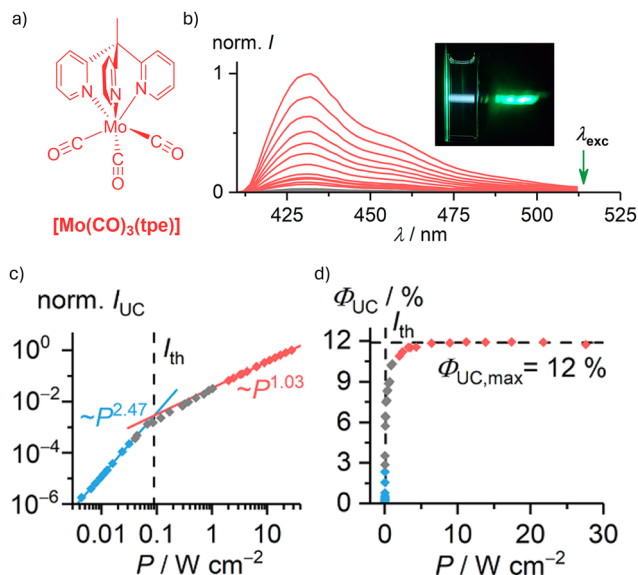
This journal is © the Owner Societies 2025

Phys. Chem. Chem. Phys., 2025, **27**, 13793–13811 | **13805**

Fig. 13 Green-to-blue upconversion sensitized by [Mo(CO)₃(tpe)] with DPA as the annihilator. (a) Molecular structure of [Mo(CO)₃(tpe)]. (b) Upconversion luminescence spectra recorded from a [Mo(CO)₃(tpe)] solution containing 10 mM DPA in deaerated THF following CW-laser excitation at 514 nm with different power densities. Inset: Photographs of the green excitation light (right) and blue upconverted emission (left). (c) Doubly logarithmic plot of the integrated upconverted fluorescence intensity I_{UC} vs. laser power density P. I_{th} is the threshold excitation power density. (d) Upconversion quantum yield Φ_{UC} (theoretical maximal Φ_{UC} is set to 50%[54]) as a function of the excitation power density P.[158] (b)–(d) Reproduced with permission from ref. 158. Copyright 2023, American Chemical Society.

commonly long-lived triplet metal-to-ligand charge transfer (³MLCT) excited states, photoactive earth-abundant metal complexes often exhibit more labile and sophisticated excited state landscapes with distinct electronic structures and uncommon spin states. This often leads to short excited state lifetimes that kinetically hinder the diffusional encounter with an annihilator and therefore undermine their performance in photon upconversion, which is particularly true for 3d⁵ Fe(III)[31,36] as well as 3d⁶ Cr(0)[27,167] and Mn(I)[116] complexes.

To address these fundamental challenges, rationalized molecular design guidelines are needed for these earth-abundant transition metals, as currently being explored by many coordination chemists.[91–98] In parallel, deliberate sTTA-UC design concepts have been shown to boost the reactivity of these novel metal complexes and improve their upconversion performance, such as preassociation of the photosensitizer/annihilator pair to circumvent diffusional encounter or introducing a mediator with a long excited state lifetime to enhance the dynamic energy transfer.[36,241,242] Driven by the photon upconversion sensitized by earth-abundant metal complexes, energy transfer- and photoredox catalysis, such as photodimerization,[166] photopolymerizations[23,27,36] and photoisomerization,[157] are achieved with low-energy visible light.

Our recent sTTA-UC studies with doublet photosensitizers based on 3d³ Cr(III) and 3d⁵ low-spin Fe(III) reported unusual doublet–triplet energy transfer (DTET) mechanisms,[36,112,166,193]

similar to the DTET explored with doublet organic radicals for sTTA-UC.[84–86] Differing from the conventional understanding of triplet–triplet energy transfer dynamics, these findings open the door of utilizing metal complexes featuring doublet excited states for photon upconversion and energy transfer-based applications. Collectively, these studies offer an important fundamental understanding of the photophysical behavior for earth-abundant metal complexes and indicate their bright future as photosensitizers in the fields of photon upconversion, light harvesting, and photocatalysis.

Data availability

No primary research results, software or code have been included and no new data were generated or analysed as part of this review.

Conflicts of interest

The authors declare no conflicts of interest.

Acknowledgements

Notes and references

1 C. A. Parker and C. G. Hatchard, *Proc. Chem. Soc.*, 1962, 386–387.

2 C. A. Parker, C. G. Hatchard and T. A. Joyce, *Nature*, 1965, **205**, 1282–1284.

3 T. N. Singh-Rachford and F. N. Castellano, *Coord. Chem. Rev.*, 2010, **254**, 2560–2573.

4 V. Gray, K. Moth-Poulsen, B. Albinsson and M. Abrahamsson, *Coord. Chem. Rev.*, 2018, **362**, 54–71.

5 Q. Dou, L. Jiang, D. Kai, C. Owh and X. J. Loh, *Drug Discovery Today*, 2017, **22**, 1400–1411.

6 Q. Liu, M. Xu, T. Yang, B. Tian, X. Zhang and F. Li, *ACS Appl. Mater. Interfaces*, 2018, **10**, 9883–9888.

7 Z.-S. Yang, Y. Ning, H.-Y. Yin and J.-L. Zhang, *Inorg. Chem. Front.*, 2018, **5**, 2291–2299.

8 L. Huang, E. Kakadiaris, T. Vaneckova, K. Huang, M. Vaculovicova and G. Han, *Biomaterials*, 2019, **201**, 77–86.

9 L. Huang, T. Le, K. Huang and G. Han, *Nat. Commun.*, 2021, **12**, 1898.

10 T. Schloemer, P. Narayanan, Q. Zhou, E. Belliveau, M. Seitz and D. N. Congreve, *ACS Nano*, 2023, **17**, 3259–3288.

11 W. Lin, J. Li, H. Feng, F. Qi and L. Huang, *J. Anal. Test.*, 2023, **7**, 327–344.

12 A. Prabhakaran, K. K. Jha, R. C. E. Sia, R. A. Arellano Reyes, N. K. Sarangi, M. Kogut, J. Guthmuller, J. Czub, B. Dietzek-Ivanšić and T. E. Keyes, *ACS Appl. Mater. Interfaces*, 2024, **16**, 29324–29337.

13806 | *Phys. Chem. Chem. Phys.*, 2025, **27**, 13793–13811

This journal is © the Owner Societies 2025

13 T. F. Schulze and T. W. Schmidt, *Energy Environ. Sci.*, 2015, **8**, 103–125.

14 T. Dilbeck and K. Hanson, *J. Phys. Chem. Lett.*, 2018, **9**, 5810–5821.

15 B. S. Richards, D. Hudry, D. Busko, A. Turshatov and I. A. Howard, *Chem. Rev.*, 2021, **121**, 9165–9195.

16 S. E. Seo, H.-S. Choe, H. Cho, H.-I. Kim, J.-H. Kim and O. S. Kwon, *J. Mater. Chem. C*, 2022, **10**, 4483–4496.

17 A. J. Carrod, V. Gray and K. Börjesson, *Energy Environ. Sci.*, 2022, **15**, 4982–5016.

18 D. Y. Kondakov, *Philos. Trans. R. Soc., A*, 2015, **373**, 20140321.

19 C. Gao, W. W. H. Wong, Z. Qin, S.-C. Lo, E. B. Namdas, H. Dong and W. Hu, *Adv. Mater.*, 2021, **33**, 2100704.

20 X. Cao, K. Pan, J. Miao, X. Lv, Z. Huang, F. Ni, X. Yin, Y. Wei and C. Yang, *J. Am. Chem. Soc.*, 2022, **144**, 22976–22984.

21 J. Zhou, Q. Liu, W. Feng, Y. Sun and F. Li, *Chem. Rev.*, 2015, **115**, 395–465.

22 P. Bharmoria, H. Bildirir and K. Moth-Poulsen, *Chem. Soc. Rev.*, 2020, **49**, 6529–6554.

23 N. Awwad, A. T. Bui, E. O. Danilov and F. N. Castellano, *Chem*, 2020, **6**, 3071–3085.

24 F. Glaser, C. Kerzig and O. S. Wenger, *Chem. Sci.*, 2021, **12**, 9922–9933.

25 R. Pérez-Ruiz, *Top. Curr. Chem.*, 2022, **380**, 23.

26 S. N. Sanders, T. H. Schloemer, M. K. Gangishetty, D. Anderson, M. Seitz, A. O. Gallegos, R. C. Stokes and D. N. Congreve, *Nature*, 2022, **604**, 474–478.

27 C. Wang, C. Wegeberg and O. S. Wenger, *Angew. Chem., Int. Ed.*, 2023, **62**, e202311470.

28 H. Li, C. Wang, F. Glaser, N. Sinha and O. S. Wenger, *J. Am. Chem. Soc.*, 2023, **145**, 11402–11414.

29 N. Sinha, C. Wegeberg, D. Häussinger, A. Prescimone and O. S. Wenger, *Nat. Chem.*, 2023, **15**, 1730–1736.

30 M. Uji, T. J. B. Zähringer, C. Kerzig and N. Yanai, *Angew. Chem., Int. Ed.*, 2023, **62**, e202301506.

31 J. Wellauer, F. Ziereisen, N. Sinha, A. Prescimone, A. Velić, F. Meyer and O. S. Wenger, *J. Am. Chem. Soc.*, 2024, **146**, 11299–11318.

32 L. Huang and G. Han, *Nat. Rev. Chem.*, 2024, **8**, 238–255.

33 W. Yao, X. Song, L. Xue, S. Liu, L. Tang, Y. Chen, H. Liu and X. Li, *ChemPhotoChem*, 2024, **8**, e202400184.

34 L. R. Beck, K. A. Xie, B. C. Lainhart, T. C. Sherwood, E. R. Welin, C. L. Joe and T. Rovis, *ACS Catal.*, 2024, **14**, 18515–18522.

35 H. Hammecke, D. Fritzler, N. Vashistha, P. Jin, B. Dietzek-Ivanšić and C. Wang, *Chem. - Eur. J.*, 2024, **30**, e202402679.

36 P. Jin, X. Xu, Y. Yan, H. Hammecke and C. Wang, *J. Am. Chem. Soc.*, 2024, **146**, 35390–35401.

37 D. Yildiz, C. Baumann, A. Mikosch, A. J. C. Kuehne, A. Herrmann and R. Göstl, *Angew. Chem., Int. Ed.*, 2019, **58**, 12919–12923.

38 K. Ye, M. Imran, X. Chen and J. Zhao, *ACS Appl. Opt. Mater.*, 2024, **2**, 1803–1824.

39 C. A. Parker and C. G. Hatchard, *Proc. Math. Phys. Eng. Sci.*, 1962, **269**, 574–584.

40 T. C. Wu, D. N. Congreve and M. A. Baldo, *Appl. Phys. Lett.*, 2015, **107**, 031103.

41 J. Peng, X. Guo, X. Jiang, D. Zhao and Y. Ma, *Chem. Sci.*, 2016, **7**, 1233–1237.

42 N. Yanai, M. Kozue, S. Amemori, R. Kabe, C. Adachi and N. Kimizuka, *J. Mater. Chem. C*, 2016, **4**, 6447–6451.

43 N. Yanai and N. Kimizuka, *Acc. Chem. Res.*, 2017, **50**, 2487–2495.

44 T. J. B. Zähringer, J. A. Moghtader, M. S. Bertrams, B. Roy, M. Uji, N. Yanai and C. Kerzig, *Angew. Chem., Int. Ed.*, 2023, **62**, e202215340.

45 M. Zheng, Y. Li, Y. Wei, L. Chen, S. Liu and X. Zhou, *J. Phys. Chem. C*, 2023, **127**, 2846–2854.

46 A. Olesund, J. Johnsson, F. Edhborg, S. Ghasemi, K. Moth-Poulsen and B. Albinsson, *J. Am. Chem. Soc.*, 2022, **144**, 3706–3716.

47 D. Liu, Y. Zhao, Z. Wang, K. Xu and J. Zhao, *Dalton Trans.*, 2018, **47**, 8619–8628.

48 Y. Wei, M. Zheng, L. Chen, X. Zhou and S. Liu, *Dalton Trans.*, 2019, **48**, 11763–11771.

49 D. Beery, A. Arcidiacono, J. P. Wheeler, J. Chen and K. Hanson, *J. Mater. Chem. C*, 2022, **10**, 4947–4954.

50 Z. Yuan, J. He, Z. Mahmood, L. Xing, S. Ji, Y. Huo and H.-L. Zhang, *Dyes Pigm.*, 2022, **199**, 110049.

51 Y. Sasaki, M. Oshikawa, P. Bharmoria, H. Kouno, A. Hayashi-Takagi, M. Sato, I. Ajioka, N. Yanai and N. Kimizuka, *Angew. Chem., Int. Ed.*, 2019, **58**, 17827–17833.

52 Y. Sasaki, N. Yanai and N. Kimizuka, *Inorg. Chem.*, 2022, **61**, 5982–5990.

53 D. G. Bossanyi, Y. Sasaki, S. Wang, D. Chekulaev, N. Kimizuka, N. Yanai and J. Clark, *JACS Au*, 2021, **1**, 2188–2201.

54 Y. Zhou, F. N. Castellano, T. W. Schmidt and K. Hanson, *ACS Energy Lett.*, 2020, **5**, 2322–2326.

55 A. Monguzzi, R. Tubino, S. Hoseinkhani, M. Campione and F. Meinardi, *Phys. Chem. Chem. Phys.*, 2012, **14**, 4322–4332.

56 V. Gray, A. Dreos, P. Erhart, B. Albinsson, K. Moth-Poulsen and M. Abrahamsson, *Phys. Chem. Chem. Phys.*, 2017, **19**, 10931–10939.

57 A. Haefele, J. Blumhoff, R. S. Khnayzer and F. N. Castellano, *J. Phys. Chem. Lett.*, 2012, **3**, 299–303.

58 F. Edhborg, A. Olesund and B. Albinsson, *Photochem. Photobiol. Sci.*, 2022, **21**, 1143–1158.

59 A. Monguzzi, J. Mezyk, F. Scotognella, R. Tubino and F. Meinardi, *Phys. Rev. B: Condens. Matter Mater. Phys.*, 2008, **78**, 195112.

60 U. Resch-Genger and H. H. Gorris, *Anal. Bioanal. Chem.*, 2017, **409**, 5855–5874.

61 L. M. Wiesholler, F. Frenzel, B. Grauel, C. Wurth, U. Resch-Genger and T. Hirsch, *Nanoscale*, 2019, **11**, 13440–13449.

62 R. Marin, D. Jaque and A. Benayas, *Nanoscale Horiz.*, 2021, **6**, 209–230.

63 T. J. B. Zähringer, M.-S. Bertrams and C. Kerzig, *J. Mater. Chem. C*, 2022, **10**, 4568–4573.

64 S. Baluschev, K. Katta, Y. Avlasevich and K. Landfester, *Mater. Horiz.*, 2016, **3**, 478–486.

65 S. H. C. Askes and S. Bonnet, *Nat. Rev. Chem.*, 2018, **2**, 437–452.

This journal is © the Owner Societies 2025

Phys. Chem. Chem. Phys., 2025, **27**, 13793–13811 | **13807**

66 H. Zhou, J. Lin, S. Wan and W. Lu, *Phys. Chem. Chem. Phys.*, 2022, **24**, 29151–29158.

67 P. Duan, N. Yanai and N. Kimizuka, *J. Am. Chem. Soc.*, 2013, **135**, 19056–19059.

68 T. Ogawa, N. Yanai, A. Monguzzi and N. Kimizuka, *Sci. Rep.*, 2015, **5**, 10882.

69 P. W. Zach, S. A. Freunberger, I. Klimant and S. M. Borisov, *ACS Appl. Mater. Interfaces*, 2017, **9**, 38008–38023.

70 D. Dzebo, K. Moth-Poulsen and B. Albinsson, *Photochem. Photobiol. Sci.*, 2017, **16**, 1327–1334.

71 N. Nishimura, V. Gray, J. R. Allardice, Z. Zhang, A. Pershin, D. Beljonne and A. Rao, *ACS Mater. Lett.*, 2019, **1**, 660–664.

72 C. Fan, L. Wei, T. Niu, M. Rao, G. Cheng, J. J. Chruma, W. Wu and C. Yang, *J. Am. Chem. Soc.*, 2019, **141**, 15070–15077.

73 S. Gharaati, C. Wang, C. Förster, F. Weigert, U. Resch-Genger and K. Heinze, *Chem. - Eur. J.*, 2020, **26**, 1003–1007.

74 M. Kanoh, Y. Matsui, K. Honda, Y. Kokita, T. Ogaki, E. Ohta and H. Ikeda, *J. Phys. Chem. B*, 2021, **125**, 4831–4837.

75 W. Wu, S. Ji, W. Wu, J. Shao, H. Guo, T. D. James and J. Zhao, *Chem. - Eur. J.*, 2012, **18**, 4953–4964.

76 P. C. Boutin, K. P. Ghiggino, T. L. Kelly and R. P. Steer, *J. Phys. Chem. Lett.*, 2013, **4**, 4113–4118.

77 C. Kerzig and O. S. Wenger, *Chem. Sci.*, 2018, **9**, 6670–6678.

78 A. C. Sell, J. C. Wetzel, M. Schmitz, A. W. Maijenburg, G. Woltersdorf, R. Naumann and C. Kerzig, *Dalton Trans.*, 2022, **51**, 10799–10808.

79 J. Sun, F. Zhong, X. Yi and J. Zhao, *Inorg. Chem.*, 2013, **52**, 6299–6310.

80 J. Peng, X. Jiang, X. Guo, D. Zhao and Y. Ma, *Chem. Commun.*, 2014, **50**, 7828–7830.

81 S. Amemori, Y. Sasaki, N. Yanai and N. Kimizuka, *J. Am. Chem. Soc.*, 2016, **138**, 8702–8705.

82 Y. Sasaki, S. Amemori, H. Kouno, N. Yanai and N. Kimizuka, *J. Mater. Chem. C*, 2017, **5**, 5063–5067.

83 Y. Wei, Y. Li, M. Zheng, X. Zhou, Y. Zou and C. Yang, *Adv. Opt. Mater.*, 2020, **8**, 1902157.

84 J. M. O'Shea, Y. J. Yun, A. M. Jamhawi, F. Peccati, G. Jimenez-Oses and A. J. Ayitou, *J. Am. Chem. Soc.*, 2025, **147**, 1017–1027.

85 J. Han, Y. Jiang, A. Obolda, P. Duan, F. Li and M. Liu, *J. Phys. Chem. Lett.*, 2017, **8**, 5865–5870.

86 Y. Wei, K. An, X. Xu, Z. Ye, X. Yin, X. Cao and C. Yang, *Adv. Opt. Mater.*, 2024, **12**, 2301134.

87 Z. Wang and J. Zhao, *Org. Lett.*, 2017, **19**, 4492–4495.

88 R. A. Arellano-Reyes, A. Prabhakaran, R. C. E. Sia, J. Guthmuller, K. K. Jha, T. Yang, B. Dietzek-Ivanšić, V. McKee and T. E. Keyes, *Chem. - Eur. J.*, 2023, **29**, e202300239.

89 Y. Li, J. Zhang, S. E. Zhu, Y. Wei, F. Zhang, L. Chen, X. Zhou and S. Liu, *J. Phys. Chem. B*, 2023, **127**, 8476–8486.

90 X. Zhang, Z. Wang, Y. Hou, Y. Yan, J. Zhao and B. Dick, *J. Mater. Chem. C*, 2021, **9**, 11944–11973.

91 V. W.-W. Yam and W.-K. Kwok, in *Advances in Inorganic Chemistry*, ed. R. van Eldik and P. C. Ford, Academic Press, 2024, vol. 83, pp. 1–31.

92 M. Kato, in *Advances in Inorganic Chemistry*, ed. R. van Eldik and P. C. Ford, Academic Press, 2024, vol. 83, pp. 33–62.

93 P. S. Wagenknecht, in *Advances in Inorganic Chemistry*, ed. R. van Eldik and P. C. Ford, Academic Press, 2024, vol. 83, pp. 63–109.

94 C. Förster and K. Heinze, in *Advances in Inorganic Chemistry*, ed. R. van Eldik and P. C. Ford, Academic Press, 2024, vol. 83, pp. 111–159.

95 B. Thomas and A. J. Morris, in *Advances in Inorganic Chemistry*, ed. R. van Eldik and P. C. Ford, Academic Press, 2024, vol. 83, pp. 161–187.

96 J. Schaab, P. I. Djurovich and M. E. Thompson, in *Advances in Inorganic Chemistry*, ed. R. van Eldik and P. C. Ford, Academic Press, 2024, vol. 83, pp. 189–221.

97 M. V. Appleby, R. A. Cowin and J. A. Weinstein, in *Advances in Inorganic Chemistry*, ed. R. van Eldik and P. C. Ford, Academic Press, 2024, vol. 83, pp. 223–267.

98 P. C. Ford, in *Advances in Inorganic Chemistry*, ed. R. van Eldik and P. C. Ford, Academic Press, 2024, vol. 83, pp. 269–303.

99 V. Ferraro, C. Bizzarri and S. Bräse, *Adv. Sci.*, 2024, **11**, 2404866.

100 R. D. Dill, R. I. Portillo, S. G. Shepard, M. P. Shores, A. K. Rappé and N. H. Damrauer, *Inorg. Chem.*, 2020, **59**, 14706–14715.

101 M. Dorn, J. Kalmbach, P. Boden, A. Papcke, S. Gomez, C. Förster, F. Kuczelinis, L. M. Carrella, L. A. Büldt, N. H. Bings, E. Rentschler, S. Lochbrunner, L. Gonzalez, M. Gerhards, M. Seitz and K. Heinze, *J. Am. Chem. Soc.*, 2020, **142**, 7947–7955.

102 M. Dorn, J. Kalmbach, P. Boden, A. Kruse, C. Dab, C. Reber, G. Niedner-Schatteburg, S. Lochbrunner, M. Gerhards, M. Seitz and K. Heinze, *Chem. Sci.*, 2021, **12**, 10780–10790.

103 J. P. Zobel, T. Knoll and L. González, *Chem. Sci.*, 2021, **12**, 10791–10801.

104 M. Dorn, D. Hunger, C. Förster, R. Naumann, J. van Slageren and K. Heinze, *Chem. - Eur. J.*, 2023, **29**, e202202898.

105 S. Otto, M. Grabolle, C. Förster, C. Kreitner, U. Resch-Genger and K. Heinze, *Angew. Chem., Int. Ed.*, 2015, **54**, 11572–11576.

106 C. Wang, S. Otto, M. Dorn, E. Kreidt, J. Lebon, L. Srsan, P. Di Martino-Fumo, M. Gerhards, U. Resch-Genger, M. Seitz and K. Heinze, *Angew. Chem., Int. Ed.*, 2018, **57**, 1112–1116.

107 S. Treiling, C. Wang, C. Förster, F. Reichenauer, J. Kalmbach, P. Boden, J. P. Harris, L. M. Carrella, E. Rentschler, U. Resch-Genger, C. Reber, M. Seitz, M. Gerhards and K. Heinze, *Angew. Chem., Int. Ed.*, 2019, **58**, 18075–18085.

108 J.-R. Jiménez, B. Doistau, C. M. Cruz, C. Besnard, J. M. Cuerva, A. G. Campaña and C. Piguet, *J. Am. Chem. Soc.*, 2019, **141**, 13244–13252.

109 F. Reichenauer, C. Wang, C. Förster, P. Boden, N. Ugur, R. Báez-Cruz, J. Kalmbach, L. M. Carrella, E. Rentschler, C. Ramanan, G. Niedner-Schatteburg, M. Gerhards, M. Seitz, U. Resch-Genger and K. Heinze, *J. Am. Chem. Soc.*, 2021, **143**, 11843–11855.

110 N. Sinha, J. R. Jimenez, B. Pfund, A. Prescimone, C. Piguet and O. S. Wenger, *Angew. Chem., Int. Ed.*, 2021, **60**, 23722–23728.

13808 | *Phys. Chem. Chem. Phys.*, 2025, **27**, 13793–13811

This journal is © the Owner Societies 2025

111 C. Wegeberg, D. Häussinger and O. S. Wenger, *J. Am. Chem. Soc.*, 2021, **143**, 15800–15811.

112 S. Trippmacher, S. Demeshko, A. Prescimone, F. Meyer, O. S. Wenger and C. Wang, *Chem. - Eur. J.*, 2024, **30**, e202400856.

113 F. Reichenauer, R. Naumann, C. Förster, W. R. Kitzmann, A.-P. M. Reponen, S. Feldmann and K. Heinze, *Chem. Sci.*, 2024, **15**, 20251–20262.

114 F. Reichenauer, D. Zorn, R. Naumann, C. Förster and K. Heinze, *Inorg. Chem.*, 2024, **63**, 23487–23496.

115 N. R. East, R. Naumann, C. Förster, C. Ramanan, G. Diezemann and K. Heinze, *Nat. Chem.*, 2024, **16**, 827–834.

116 P. Herr, C. Kerzig, C. B. Larsen, D. Häussinger and O. S. Wenger, *Nat. Chem.*, 2021, **13**, 956–962.

117 C. Wegeberg, D. Häussinger, S. Kupfer and O. S. Wenger, *J. Am. Chem. Soc.*, 2024, **146**, 4605–4619.

118 T. Huang, P. Du, X. Cheng and Y. M. Lin, *J. Am. Chem. Soc.*, 2024, **146**, 24515–24525.

119 N. Kaul, E. Asempa, J. A. Valdez-Moreira, J. M. Smith, E. Jakubikova and L. Hammarström, *J. Am. Chem. Soc.*, 2024, **146**, 24619–24629.

120 K. S. Kjær, N. Kaul, O. Prakash, P. Chábera, N. W. Rosemann, A. Honarfar, O. Gordivska, L. A. Fredin, K.-E. Bergquist, L. Häggström, T. Ericsson, L. Lindh, A. Yartsev, S. Styring, P. Huang, J. Uhlig, J. Bendix, D. Strand, V. Sundström, P. Persson, R. Lomoth and K. Wärnmark, *Science*, 2019, **363**, 249–253.

121 J. D. Braun, I. B. Lozada, C. Kolodziej, C. Burda, K. M. E. Newman, J. van Lierop, R. L. Davis and D. E. Herbert, *Nat. Chem.*, 2019, **11**, 1144–1150.

122 J. Steube, A. Kruse, O. S. Bokareva, T. Reuter, S. Demeshko, R. Schoch, M. A. Arguello Cordero, A. Krishna, S. Hohloch, F. Meyer, K. Heinze, O. Kühn, S. Lochbrunner and M. Bauer, *Nat. Chem.*, 2023, **15**, 468–474.

123 J. T. Malme, R. A. Clendening, R. Ash, T. Curry, T. Ren and J. Vura-Weis, *J. Am. Chem. Soc.*, 2023, **145**, 6029–6034.

124 Y. Ye, P. Garrido-Barros, J. Wellauer, C. M. Cruz, R. Lescouëzec, O. S. Wenger, J. M. Herrera and J. R. Jiménez, *J. Am. Chem. Soc.*, 2024, **146**, 954–960.

125 T. Reuter, D. Zorn, R. Naumann, J. Klett, C. Förster and K. Heinze, *Angew. Chem., Int. Ed.*, 2024, **63**, e202406438.

126 L. Lindh, N. W. Rosemann, I. B. Losada, S. Persson, Y. Goriya, H. Fan, O. Gordivska, K. Wärnmark, J. Uhlig, P. Chábera, A. Yartsev and P. Persson, *Coord. Chem. Rev.*, 2024, **506**, 215709.

127 N. Sinha, J. Wellauer, T. Maisuradze, A. Prescimone, S. Kupfer and O. S. Wenger, *J. Am. Chem. Soc.*, 2024, **146**, 10418–10431.

128 R. J. Ortiz, R. Mondal, J. K. McCusker and D. E. Herbert, *J. Am. Chem. Soc.*, 2025, **147**, 1694–1708.

129 F. Glaser, S. De Kreijger and L. Troian-Gautier, *J. Am. Chem. Soc.*, 2025, **147**, 8559–8567.

130 J. Wellauer, B. Pfund, I. Becker, F. Meyer, A. Prescimone and O. S. Wenger, *J. Am. Chem. Soc.*, 2025, **147**, 8760–8768.

131 A. K. Pal, C. Li, G. S. Hanan and E. Zysman-Colman, *Angew. Chem., Int. Ed.*, 2018, **57**, 8027–8031.

132 N. Sinha, B. Pfund, C. Wegeberg, A. Prescimone and O. S. Wenger, *J. Am. Chem. Soc.*, 2022, **144**, 9859–9873.

133 M. M. Alowakennu, A. Ghosh and J. K. McCusker, *J. Am. Chem. Soc.*, 2023, **145**, 20786–20791.

134 A. Y. Chan, A. Ghosh, J. T. Yarranton, J. Twilton, J. Jin, D. M. Arias-Rotondo, H. A. Sakai, J. K. McCusker and D. W. C. MacMillan, *Science*, 2023, **382**, 191–197.

135 Y. S. Wong, M. C. Tang, M. Ng and V. W. Yam, *J. Am. Chem. Soc.*, 2020, **142**, 7638–7646.

136 S. I. Ting, S. Garakyaraghi, C. M. Taliaferro, B. J. Shields, G. D. Scholes, F. N. Castellano and A. G. Doyle, *J. Am. Chem. Soc.*, 2020, **142**, 5800–5810.

137 T. Ogawa, N. Sinha, B. Pfund, A. Prescimone and O. S. Wenger, *J. Am. Chem. Soc.*, 2022, **144**, 21948–21960.

138 T. Ogawa and O. S. Wenger, *Angew. Chem., Int. Ed.*, 2023, **62**, e202312851.

139 E. Sutcliffe, D. A. Cagan and R. G. Hadt, *J. Am. Chem. Soc.*, 2024, **146**, 15506–15514.

140 M. Gao, W.-P. To, G. S. M. Tong, L. Du, K.-H. Low, Z. Tang, W. Lu and C.-M. Che, *Angew. Chem., Int. Ed.*, 2025, **64**, e202414411.

141 C. E. McCusker and F. N. Castellano, *Inorg. Chem.*, 2015, **54**, 6035–6042.

142 A. Hossain, A. Bhattacharyya and O. Reiser, *Science*, 2019, **364**, eaav9713.

143 R. Hamze, J. L. Peltier, D. Sylvinson, M. Jung, J. Cardenas, R. Haiges, M. Soleilhavoup, R. Jazzar, P. I. Djurovich, G. Bertrand and M. E. Thompson, *Science*, 2019, **363**, 601–606.

144 R. Fayad, A. T. Bui, S. G. Shepard and F. N. Castellano, *ACS Appl. Energy Mater.*, 2020, **3**, 12557–12564.

145 M. Gernert, L. Balles-Wolf, F. Kerner, U. Müller, A. Schmiedel, M. Holzapfel, C. M. Marian, J. Pflaum, C. Lambert and A. Steffen, *J. Am. Chem. Soc.*, 2020, **142**, 8897–8909.

146 Y. Yang, F. Doettinger, C. Kleeberg, W. Frey, M. Karnahl and S. Tschierlei, *Front. Chem.*, 2022, **10**, 936863.

147 F. Doettinger, Y. Yang, M. Karnahl and S. Tschierlei, *Inorg. Chem.*, 2023, **62**, 8166–8178.

148 D. Kim, M. C. Rosko, F. N. Castellano, T. G. Gray and T. S. Teets, *J. Am. Chem. Soc.*, 2024, **146**, 19193–19204.

149 F. N. Castellano and M. C. Rosko, *Acc. Chem. Res.*, 2024, **57**, 2872–2886.

150 C. Bizzarri, *Eur. J. Org. Chem.*, 2022, e202200185.

151 C. Bruschi, X. Gui, O. Fuhr, W. Klopper and C. Bizzarri, *Dalton Trans.*, 2023, **52**, 7809–7818.

152 J. A. Kübler, B. Pfund and O. S. Wenger, *JACS Au*, 2022, **2**, 2367–2380.

153 O. Mrózek, M. Mitra, B. Hupp, A. Belyaev, N. Lüdtke, D. Wagner, C. Wang, O. S. Wenger, C. M. Marian and A. Steffen, *Chem. - Eur. J.*, 2023, **29**, e202203980.

154 M. Mitra, O. Mrózek, M. Putscher, J. Guhl, B. Hupp, A. Belyaev, C. M. Marian and A. Steffen, *Angew. Chem., Int. Ed.*, 2024, **63**, e202316300.

155 Y. Zhang, T. S. Lee, J. L. Petersen and C. Milsmann, *J. Am. Chem. Soc.*, 2018, **140**, 5934–5947.

156 Y. Zhang, T. S. Lee, J. M. Favale, D. C. Leary, J. L. Petersen, G. D. Scholes, F. N. Castellano and C. Milsmann, *Nat. Chem.*, 2020, **12**, 345–352.

This journal is © the Owner Societies 2025

Phys. Chem. Chem. Phys., 2025, **27**, 13793–13811 | **13809**

157 J. B. Bilger, C. Kerzig, C. B. Larsen and O. S. Wenger, *J. Am. Chem. Soc.*, 2021, **143**, 1651–1663.

158 W. R. Kitzmann, M. S. Bertrams, P. Boden, A. C. Fischer, R. Klauer, J. Sutter, R. Naumann, C. Förster, G. Niedner-Schatteburg, N. H. Bings, J. Hunger, C. Kerzig and K. Heinze, *J. Am. Chem. Soc.*, 2023, **145**, 16597–16609.

159 W. R. Kitzmann, D. Hunger, A. M. Reponen, C. Förster, R. Schoch, M. Bauer, S. Feldmann, J. van Slageren and K. Heinze, *Inorg. Chem.*, 2023, **62**, 15797–15808.

160 T. Jin, D. Wagner and O. S. Wenger, *Angew. Chem., Int. Ed.*, 2024, **63**, e202314475.

161 T. Jin, N. Sinha, D. S. Wagner, A. Prescimone, D. Häussinger and O. S. Wenger, *J. Am. Chem. Soc.*, 2025, **147**, 4587–4594.

162 A. C. Fischer, C. Förster, W. R. Kitzmann and K. Heinze, *Inorg. Chem.*, 2025, **64**, 6100–6114.

163 C. Förster and K. Heinze, *Chem. Soc. Rev.*, 2020, **49**, 1057–1070.

164 C. E. Housecroft and E. C. Constable, *Chem. Sci.*, 2022, **13**, 1225–1262.

165 N. Sinha and O. S. Wenger, *J. Am. Chem. Soc.*, 2023, **145**, 4903–4920.

166 C. Wang, F. Reichenauer, W. R. Kitzmann, C. Kerzig, K. Heinze and U. Resch-Genger, *Angew. Chem., Int. Ed.*, 2022, **61**, e202202238.

167 L. A. Büldt, X. Guo, R. Vogel, A. Prescimone and O. S. Wenger, *J. Am. Chem. Soc.*, 2017, **139**, 985–992.

168 J. A. O'Brien, S. Rallabandi, U. Tripathy, M. F. Paige and R. P. Steer, *Chem. Phys. Lett.*, 2009, **475**, 220–222.

169 S. K. Sugunan, U. Tripathy, S. M. K. Brunet, M. F. Paige and R. P. Steer, *J. Phys. Chem. A*, 2009, **113**, 8548–8556.

170 X. Cui, J. Zhao, P. Yang and J. Sun, *Chem. Commun.*, 2013, **49**, 10221–10223.

171 R. Rautela, N. K. Joshi, S. Novakovic, W. W. H. Wong, J. M. White, K. P. Ghiggino, M. F. Paige and R. P. Steer, *Phys. Chem. Chem. Phys.*, 2017, **19**, 23471–23482.

172 N. A. Durandin, J. Isokuortti, A. Efimov, E. Vuorimaa-Laukkanen, N. V. Tkachenko and T. Laaksonen, *Chem. Commun.*, 2018, **54**, 14029–14032.

173 K. M. Felter, M. C. Fravventura, E. Koster, R. D. Abellon, T. J. Savenije and F. C. Grozema, *ACS Energy Lett.*, 2020, **5**, 124–129.

174 Z. Mahmood, N. Rehmat, S. Ji, J. Zhao, S. Sun, M. Di Donato, M. Li, M. Teddei and Y. Huo, *Chemistry*, 2020, **26**, 14912–14918.

175 M. Yang, S. Sheykhi, Y. Zhang, C. Milsmann and F. N. Castellano, *Chem. Sci.*, 2021, **12**, 9069–9077.

176 S. Otto, M. Dorn, C. Förster, M. Bauer, M. Seitz and K. Heinze, *Coord. Chem. Rev.*, 2018, **359**, 102–111.

177 W. R. Kitzmann, J. Moll and K. Heinze, *Photochem. Photobiol. Sci.*, 2022, **21**, 1309–1331.

178 J. R. Jiménez, M. Poncet, S. Miguez-Lago, S. Grass, J. Lacour, C. Besnard, J. M. Cuerva, A. G. Campaña and C. Piguet, *Angew. Chem., Int. Ed.*, 2021, **60**, 10095–10102.

179 Y. Cheng, Q. Yang, J. He, W. Zou, K. Liao, X. Chang, C. Zou and W. Lu, *Dalton Trans.*, 2023, **52**, 2561–2565.

180 T. H. Bürgin, F. Glaser and O. S. Wenger, *J. Am. Chem. Soc.*, 2022, **144**, 14181–14194.

181 S. Sittel, R. Naumann and K. Heinze, *Front. Chem.*, 2022, **10**, 887439.

182 S. Sittel, A. C. Sell, K. Hofman, C. Wiedemann, J. P. Nau, C. Kerzig, G. Manolikakes and K. Heinze, *ChemCatChem*, 2023, **15**, e202201562.

183 J. Kalmbach, C. Wang, Y. You, C. Förster, H. Schubert, K. Heinze, U. Resch-Genger and M. Seitz, *Angew. Chem., Int. Ed.*, 2020, **59**, 18804–18808.

184 F. A. Baptista, D. Krizsan, M. Stitch, I. V. Sazanovich, I. P. Clark, M. Towrie, C. Long, L. Martinez-Fernandez, R. Improta, N. A. P. Kane-Maguire, J. M. Kelly and S. J. Quinn, *J. Am. Chem. Soc.*, 2021, **143**, 14766–14779.

185 C. Förster and K. Heinze, *Chem. Phys. Rev.*, 2022, **3**, 041302.

186 W. R. Kitzmann and K. Heinze, *Angew. Chem., Int. Ed.*, 2022, **62**, e202213207.

187 C. Wang, K. Ebel, K. Heinze, U. Resch-Genger and I. Bald, *Chem. - Eur. J.*, 2023, **29**, e202203719.

188 C. Wang, H. Li, T. H. Bürgin and O. S. Wenger, *Nat. Chem.*, 2024, **16**, 1151–1159.

189 E. Wigner, *Math Physik, Kl, IIa*, 1927, 375–381.

190 A. R. Lee, C. S. Enos and A. G. Brenton, *Int. J. Mass Spectrom. Ion Processes*, 1991, **104**, 49–62.

191 K. S. Wei and R. Livingston, *Photochem. Photobiol.*, 1967, **6**, 229–232.

192 G. W. Breton and X. Vang, *J. Chem. Educ.*, 1998, **75**, 81.

193 D. Fritzler and C. Wang, *ChemPhotoChem*, 2025, e202500094.

194 J. K. Li, M. Y. Zhang, L. Zeng, L. Huang and X. Y. Wang, *Angew. Chem., Int. Ed.*, 2023, **62**, e202303093.

195 S. G. Shepard, S. M. Fatur, A. K. Rappé and N. H. Damrauer, *J. Am. Chem. Soc.*, 2016, **138**, 2949–2952.

196 P. Dierks, Y. Vukadinovic and M. Bauer, *Inorg. Chem. Front.*, 2022, **9**, 206–220.

197 K. Witas, S. S. Nair, T. Maisuradze, L. Zedler, H. Schmidt, P. Garcia-Porta, A. S. J. Rein, T. Bolter, S. Rau, S. Kupfer, B. Dietzek-Ivanšić and D. U. Sorsche, *J. Am. Chem. Soc.*, 2024, **146**, 19710–19719.

198 P. Chábera, Y. Liu, O. Prakash, E. Thyrhaug, A. E. Nahhas, A. Honarfar, S. Essén, L. A. Fredin, T. C. Harlang, K. S. Kjær, K. Handrup, F. Ericson, H. Tatsuno, K. Morgan, J. Schnadt, L. Häggström, T. Ericsson, A. Sobkowiak, S. Lidin, P. Huang, S. Styring, J. Uhlig, J. Bendix, R. Lomoth, V. Sundström, P. Persson and K. Wärnmark, *Nature*, 2017, **543**, 695–699.

199 P. Chábera, L. Lindh, N. W. Rosemann, O. Prakash, J. Uhlig, A. Yartsev, K. Wärnmark, V. Sundström and P. Persson, *Coord. Chem. Rev.*, 2021, **426**, 213517.

200 A. Aydogan, R. E. Bangle, A. Cadranel, M. D. Turlington, D. T. Conroy, E. Cauët, M. L. Singleton, G. J. Meyer, R. N. Sampaio, B. Elias and L. Troian-Gautier, *J. Am. Chem. Soc.*, 2021, **143**, 15661–15673.

201 A. Ilic, J. Schwarz, C. Johnson, L. H. M. de Groot, S. Kaufhold, R. Lomoth and K. Wärnmark, *Chem. Sci.*, 2022, **13**, 9165–9175.

202 J. Schwarz, A. Ilic, C. Johnson, R. Lomoth and K. Wärnmark, *Chem. Commun.*, 2022, **58**, 5351–5354.

13810 | *Phys. Chem. Chem. Phys.*, 2025, **27**, 13793–13811

This journal is © the Owner Societies 2025

203 L. H. M. de Groot, A. Ilic, J. Schwarz and K. Wärnmark, *J. Am. Chem. Soc.*, 2023, **145**, 9369–9388.

204 S. De Kreijger, A. Ripak, B. Elias and L. Troian-Gautier, *J. Am. Chem. Soc.*, 2024, **146**, 10286–10292.

205 A. Ripak, A. K. Vega Salgado, D. Valverde, S. Cristofaro, A. de Gary, Y. Olivier, B. Elias and L. Troian-Gautier, *J. Am. Chem. Soc.*, 2024, **146**, 22818–22828.

206 A. Ilic, B. R. Strücker, C. E. Johnson, S. Hainz, R. Lomoth and K. Wärnmark, *Chem. Sci.*, 2024, **15**, 12077–12085.

207 C. E. Johnson, J. Schwarz, M. Deegbey, O. Prakash, K. Sharma, P. Huang, T. Ericsson, L. Häggström, J. Bendix, A. K. Gupta, E. Jakubikova, K. Wärnmark and R. Lomoth, *Chem. Sci.*, 2023, **14**, 10129–10139.

208 N. Kaul and R. Lomoth, *J. Am. Chem. Soc.*, 2021, **143**, 10816–10821.

209 M. Zhang, C. E. Johnson, A. Ilic, J. Schwarz, M. B. Johansson and R. Lomoth, *J. Am. Chem. Soc.*, 2023, **145**, 19171–19176.

210 A. Farrán and K. D. Deshayes, *J. Phys. Chem.*, 1996, **100**, 3305–3307.

211 D. Guo, T. E. Knight and J. K. McCusker, *Science*, 2011, **334**, 1684–1687.

212 L. A. Büldt and O. S. Wenger, *Angew. Chem., Int. Ed.*, 2017, **56**, 5676–5682.

213 P. Boden, P. Di Martino-Fumo, T. Bens, S. Steiger, U. Albold, G. Niedner-Schatteburg, M. Gerhards and B. Sarkar, *Chemistry*, 2021, **27**, 12959–12964.

214 C. Wegeberg and O. S. Wenger, *Dalton Trans.*, 2022, **51**, 1297–1302.

215 M. Scaccaglia, M. P. Birbaumer, S. Pinelli, G. Pelosi and A. Frei, *Chem. Sci.*, 2024, **15**, 3907–3919.

216 J. K. McCusker, *Science*, 2019, **363**, 484–488.

217 C. Wegeberg and O. S. Wenger, *JACS Au*, 2021, **1**, 1860–1876.

218 R. Haruki, Y. Sasaki, K. Masutani, N. Yanai and N. Kimizuka, *Chem. Commun.*, 2020, **56**, 7017–7020.

219 F. Glaser and O. S. Wenger, *Chem. Sci.*, 2023, **14**, 149–161.

220 B. D. Ravetz, A. B. Pun, E. M. Churchill, D. N. Congreve, T. Rovis and L. M. Campos, *Nature*, 2019, **565**, 343–346.

221 A. Caron, G. Noirbent, D. Gigmes, F. Dumur and J. Lalevée, *Macromol. Rapid Commun.*, 2021, **42**, 2100047.

222 W. Liang, C. Nie, J. Du, Y. Han, G. Zhao, F. Yang, G. Liang and K. Wu, *Nat. Photonics*, 2023, **17**, 346–353.

223 S. Ossinger, A. Prescimone, D. Häussinger and O. S. Wenger, *Inorg. Chem.*, 2022, **61**, 10533–10547.

224 S. Kronenberger, R. Naumann, C. Förster, N. East, J. Klett and K. Heinze, *ChemRxiv*, 2024preprint, DOI: **10.26434/chemrxiv-2024-gzvbj**.

225 A. Lavie-Cambot, M. Cantuel, Y. Leydet, G. Jonusauskas, D. M. Bassani and N. D. McClenaghan, *Coord. Chem. Rev.*, 2008, **252**, 2572–2584.

226 M. S. Lazorski and F. N. Castellano, *Polyhedron*, 2014, **82**, 57–70.

227 O. S. Wenger, *J. Am. Chem. Soc.*, 2018, **140**, 13522–13533.

228 J. Beaudelot, S. Oger, S. Peruško, T. A. Phan, T. Teunens, C. Moucheron and G. Evano, *Chem. Rev.*, 2022, **122**, 16365–16609.

229 L. Gimeno, B. T. Phelan, E. A. Sprague-Klein, T. Roisnel, E. Blart, C. Gourlaouen, L. X. Chen and Y. Pellegrin, *Inorg. Chem.*, 2022, **61**, 7296–7307.

230 C. E. McCusker and F. N. Castellano, *Inorg. Chem.*, 2013, **52**, 8114–8120.

231 N. A. Durandin, J. Isokuortti, A. Efimov, E. Vuorimaa-Laukkanen, N. V. Tkachenko and T. Laaksonen, *J. Phys. Chem. C*, 2019, **123**, 22865–22872.

232 J. E. Rogers, K. A. Nguyen, D. C. Hufnagle, D. G. McLean, W. Su, K. M. Gossett, A. R. Burke, S. A. Vinogradov, R. Pachter and P. A. Fleitz, *J. Phys. Chem. A*, 2003, **107**, 11331.

233 M. Montalti, A. Credi, L. Prodi and M. T. Gandolfi, *Handbook of Photochemistry*, CRC Press, Boca Raton, 3rd edn, 2006.

234 D. Temerova, K. S. Kisel, T. Eskelinen, A. S. Melnikov, N. Kinnunen, P. Hirva, J. R. Shakirova, S. P. Tunik, E. V. Grachova and I. O. Koshevoy, *Inorg. Chem. Front.*, 2021, **8**, 2549–2560.

235 O. Mrózek, M. Gernert, A. Belyaev, M. Mitra, L. Janiak, C. M. Marian and A. Steffen, *Chem. - Eur. J.*, 2022, **28**, e202201114.

236 Y. Sakai, Y. Sagara, H. Nomura, N. Nakamura, Y. Suzuki, H. Miyazaki and C. Adachi, *Chem. Commun.*, 2015, **51**, 3181–3184.

237 A. S. Berezin, K. A. Vinogradova, V. P. Krivopalov, E. B. Nikolaenkova, V. F. Plyusnin, A. S. Kupryakov, N. V. Pervukhina, D. Y. Naumov and M. B. Bushuev, *Chem. - Eur. J.*, 2018, **24**, 12790–12795.

238 Y. Zhang, J. L. Petersen and C. Milsmann, *J. Am. Chem. Soc.*, 2016, **138**, 13115–13118.

239 L. A. Büldt, X. Guo, A. Prescimone and O. S. Wenger, *Angew. Chem., Int. Ed.*, 2016, **55**, 11247–11250.

240 N. Kiseleva, P. Nazari, C. Dee, D. Busko, B. S. Richards, M. Seitz, I. A. Howard and A. Turshatov, *J. Phys. Chem. Lett.*, 2020, **11**, 2477–2481.

241 L. Hou, A. Olesund, S. Thurakkal, X. Zhang and B. Albinsson, *Adv. Funct. Mater.*, 2021, **31**, 2106198.

242 F. Glaser, M. Schmitz and C. Kerzig, *Nanoscale*, 2024, **16**, 123–137.

This journal is © the Owner Societies 2025

Phys. Chem. Chem. Phys., 2025, **27**, 13793–13811 | **13811**